Mechanisms of anaphylaxis in human low-affinity IgG receptor locus knock-in mice

Caitlin M. Gillis, Friederike Jönsson, David A. Mancardi, Naxin Tu, Héloïse Beutier, Nico van Rooijen, Lynn E. Macdonald, Andrew J. Murphy, Pierre Bruhns

Mechanisms of anaphylaxis in human low-affinity IgG receptor locus knock-in mice

Caitlin M. Gillis, B.Sci.[1,2,3], Friederike Jönsson, PhD[1,2], David A. Mancardi, PhD[1,2], Naxin Tu, PhD[5], Héloïse Beutier, PharmD[1,2,3], Nico Van Rooijen, PhD[4], Lynn E. Macdonald, PhD[5], Andrew J. Murphy, PhD[5] and Pierre Bruhns, PhD[1,2]

Authors' affiliations

[1]Institut Pasteur, Department of Immunology, Unit of Antibodies in Therapy and Pathology, Paris, France;

[2]INSERM, U1222, Paris, France;

[3]Université Pierre et Marie Curie, Paris, France;

[4]Department of Molecular Cell Biology, VU Medical Center, Amsterdam, The Netherlands;

[5]Regeneron Pharmaceuticals, Inc., Tarrytown, NY, USA.

Sources of funding: *none of the sources of funding have an interest in the subject matter or materials discussed in the submitted manuscript*

Correspondence to: Pierre Bruhns and Caitlin M. Gillis, Unit of Antibodies in Therapy and Pathology, Department of Immunology, Institut Pasteur, 25 rue du Docteur Roux, 75015 Paris, France. Phone: +33144389146 or +33145688629. E-mail: bruhns@pasteur.fr; caitlin.gillis@pasteur.fr

ABSTRACT

Background: Anaphylaxis can proceed through distinct IgE- or IgG-dependant pathways, which have been investigated in various mouse models. We developed a novel mouse strain in which the human low-affinity IgG receptor locus, comprising both activating (hFcγRIIA, hFcγRIIIA, hFcγRIIIB) and inhibitory (hFcγRIIB) hFcγR genes, has been inserted into the equivalent murine locus, corresponding to a locus 'swap'.

Objective: We sought to determine the capabilities of hFcγRs to induce systemic anaphylaxis, and identify the cell types and mediators involved.

Methods: hFcγR expression on mouse and human cells was compared to validate the model. Passive systemic anaphylaxis was induced by injection of heat-aggregated human IVIG, and active systemic anaphylaxis following immunisation and challenge. Anaphylaxis severity was evaluated by hypothermia and mortality. The contribution of receptors, mediators or cell types was assessed by receptor blockade or depletion.

Results: The human to mouse low-affinity FcγR locus swap engendered hFcγRIIA/IIB/IIIA/IIIB expression in mice comparable to that in humans. Knock-in mice were susceptible to passive and active anaphylaxis, accompanied by downregulation of both activating and inhibitory hFcγR expression on specific myeloid cells. The contribution of hFcγRIIA was predominant. Depletion of neutrophils protected against hypothermia and mortality. Basophils contributed to a lesser extent. Anaphylaxis was inhibited by Platelet-Activating Factor receptor or Histamine receptor-1 blockade.

Conclusion : Low-affinity FcγR locus-switched mice represent an unprecedented model of cognate hFcγR expression. Importantly, IgG-anaphylaxis proceeds within a native context of activating and inhibitory hFcγRs; indicating that, despite robust

hFcγRIIB expression, activating signals can dominate to initiate a severe anaphylactic reaction.

CLINICAL IMPLICATIONS

In a mouse model of cognate human IgG receptors expression, hFcγR engagement with IgG immune complexes induced severe anaphylaxis. These findings benefit the understanding of human IgG-dependent anaphylaxis, whether non-classical (IgE-independent) or following IgG-based therapies.

CAPSULE SUMMARY

Antibodies of the IgG class can contribute to anaphylaxis. This report reveals that human IgG receptor knock-in mice are susceptible to systemic anaphylaxis, demonstrating the predominance of activating over inhibitory IgG receptors and the major contribution of human FcγRIIA, neutrophils and platelet-activating factor.

KEY WORDS

Anaphylaxis; IgG; knock-in mouse model; basophil; neutrophil; monocyte; macrophage; human FcγR; Platelet-activating Factor; Histamine.

ABBREVIATIONS USED

FcγR: IgG Fc receptor

PAF: Platelet-Activating Factor

WT: Wild-Type

PSA: Passive Systemic Anaphylaxis

ASA: Active Systemic Anaphylaxis

BSA: Bovine Serum Albumin

HA: heat-aggregated

mAb: monoclonal Antibody

PBS: Phosphate Buffered Saline

BBS: Borate Buffered Saline

GeoMean: Geometric Mean

SEM: Standard Error of the Mean

INTRODUCTION

Anaphylaxis is a severe, systemic allergic reaction, the reported incidence of which is increasing worldwide[1-3]. Reactions are clinically heterogeneous, yet characterised by rapid symptom progression and risk of death: intense vasodilation and bronchoconstriction can lead to hypotension, hypothermia, tachycardia, and respiratory distress, which may result in heart and lung failure. In children the most common causative agent is food, whereas in adults drug-induced anaphylaxis accounts for the majority of cases, and indeed the majority of fatal reactions. Anaphylaxis is classically attributed to an IgE-mediated reaction driven by mast cell activation and release of histamine and tryptase[4].

Many cases of human anaphylaxis, in particular to drugs, are not accompanied by elevated serum tryptase or detectable antigen-specific IgE[5-8]. Alternative, IgE-independent pathways may actually underlie a significant fraction of these anaphylactic events: indeed, non-IgE reactions have been reported to account for up to 30% of cases of drug-induced anaphylaxis[9]. Furthermore, measures of histamine and mast cell tryptase in patients' sera do not reflect the severity of reactions[7, 10], whereas serum platelet-activating factor (PAF) levels were found to directly correlate with anaphylaxis severity[11, 12]. Supporting these notions, experimental animal models have demonstrated that fatal systemic anaphylaxis following intravenous challenge proceeds via PAF release triggered by non-IgE-dependant pathways, and in particular by IgG-dependant pathways (reviewed in [13, 14]). The respective contribution of IgE- and IgG-mediated pathways in human anaphylaxis remains however to be determined.

Passive systemic anaphylaxis (PSA) may be induced in mice by the transfer of specific IgE or IgG antibodies prior to a challenge with a specific antigen, or by the transfer of pre-formed IgG immune complexes. Active systemic anaphylaxis (ASA) is elicited by immunisation with an antigen prior to challenge with the same antigen; a polyclonal IgE and IgG antibody response is generated, and death can result from antigen challenge. In both models, use of the intravenous route for allergen challenge mimics drug-induced anaphylaxis in patients. ASA does not depend on IgE antibodies, activating IgE receptors, or mast cells[15, 16], but rather requires activating IgG receptors (FcγR), and the contribution of other myeloid cells: neutrophils, basophils or monocyte/macrophages[17-19]. Platelet-activating factor (PAF) was identified as the dominant downstream mediator of IgG-induced anaphylaxis, and PAF alone, like histamine, can reproduce the signs and symptoms of anaphylaxis[20, 21]. Thus mouse models suggest a pathway of anaphylaxis driven by IgG-mediated activation of myeloid cells and relying on PAF release.

Allergic patients that possess detectable allergen-specific IgE also possess detectable allergen-specific IgG. These anti-allergen IgG antibodies are mainly of the IgG1 isotype, whereas anti-allergen IgG4 antibodies increase following allergen immunotherapy[22-25]. Allergen-specific IgG4 levels are considered a good correlate to successful allergen immunotherapy, however it remains unknown if allergen-specific IgG1 participate in, or are even responsible for, non-IgE mediated human anaphylaxis. Humans express a family of IgG receptors (FcγR), comprised of activating IgG receptors (hFcγRI/CD64, hFcγRIIA/CD32A, hFcγRIIC/CD32C, hFcγRIIIA/CD16A, hFcγRIIIB/CD16B) and a single inhibitory receptor (hFcγRIIB/CD32B), that all bind human IgG1 and that mediate most of the biological functions of IgG[26]. Although mice

also express both activating and inhibitory FcγRs, murine FcγRs do not structurally or functionally mirror those of humans: differential antibody binding affinities and variable expression on immune cell subsets prevent extrapolation from one species to another[26]. We reported previously the induction of anaphylaxis (PSA and fatal ASA) in mice transgenic either for hFcγRI/CD64 or hFcγRIIA/CD32A on a background deficient in endogenous mFcγR[19, 27]. PSA mediated by hFcγRIIA was independent of mast cells and basophils, and relied on neutrophils and monocytes/ macrophages[28], and hFcγRI-dependent ASA required neutrophils and PAF release[27]. An important caveat of these results is that they were obtained in mice expressing only one hFcγR, in the absence of potential regulatory or cooperative effects of other hFcγRs. In a model generated by intercrossing of five different hFcγR-transgenic mice, incorporating activating and inhibitory hFcγRs, administration of aggregated human IgG to [hFcγRI^{tg} hFcγRIIA^{tg} hFcγRIIB^{tg} hFcγRIIIA^{tg} hFcγRIIIB^{tg}] mice on a mFcγR^{null} background was sufficient to trigger anaphylaxis, although the mechanisms were not addressed[29]. This model reproduces, however, aberrant expressions seen in mice carrying the individual transgenes, including extremely high expression of hFcγRIIB on mouse monocytes and granulocytes[26].

Here, we present a novel mouse model in which we have employed highly efficient knock-in technology to insert the entire low-affinity hFcγR locus into the corresponding mouse locus on chromosome 1. This approach engendered expression of activating hFcγRIIA/CD32A, hFcγRIIIA/CD16A and hFcγRIIIB/CD16B, and of inhibitory hFcγRIIB/CD32B in mice, in a manner resembling expression patterns seen in humans. This unprecedented model permits analyses of the role of hFcγRs and the

cell types that express them in IgG-mediated anaphylaxis, within a cognate context of activating and inhibitory hFcγRs.

METHODS

Mice

VG1505 and VG1543 mice were designed and generated by Regeneron Pharmaceuticals, Inc. on a mixed 62.5% C57BL/6N, 37.5% 129S6/SvEv genetic background (refer to Supplemental Methods), and backcrossed one generation to C57BL/6N. Mice were bred at Institut Pasteur and used for experiments at 7-11 weeks of age. VG1505 and VG1543 mice demonstrate normal development and breeding patterns. All mouse protocols were approved by the Animal Ethics committee CETEA (Institut Pasteur, Paris, France) registered under #C2EA-89.

Active Systemic Anaphylaxis

Mice were injected intraperitoneally on day 0 with 200μg BSA in CFA, and boosted intraperitoneally on day 14 with 200μg BSA in IFA. BSA-specific IgG1, IgG2a/b/c and IgE antibodies in serum were titered by ELISA on day 21 as described[19]. Mice with comparable antibody titers were challenged intravenously with 500μg BSA 10-14 days after the last immunisation. Central temperature was monitored using a digital thermometer (YSI) with rectal probe.

Passive Systemic Anaphylaxis

Human Intravenous Immunoglobulin (IVIG; Gamunex®, Grifols) was heat-aggregated by incubation at 25mg/mL in BBS (0.17M H_3BO_3, 0.12M NaCl, pH8) for 1 hour at 63°C, then diluted in 0.9% NaCl for iv injection at 100μL per mouse. Central temperature was monitored using a digital thermometer with rectal probe. Control non-aggregated IVIG was similarly diluted without heating. For hFcγR expression analysis

following IVIG-PSA, heparinised blood was sampled 1hour after IVIG injection. IgE-dependant PSA was induced by challenge with 500μg TNP-BSA 16 hours after passive transfer of IgE anti-TNP (50μg clone C48.2). PSA was induced also by PAF injection at 0.3μg per mouse i.v., and hypothermia monitored immediately afterwards.

In vivo blocking and depletion

Anti-FcγRIIA mAbs (Clone IV.3, 60μg /mouse) were injected twice intravenously (24 hours and 4 hours) before challenge. Note that, unlike in FcγRIIA^{tg} mice [30], IV.3 administration did not induce hypothermia or symptoms of anaphylaxis, nor platelet depletion. 300μg /mouse anti-Gr-1 (RB6-8C5), 300μg /mouse anti–Ly-6G (NIMP-R14), 30μg/mouse (Supplementary Figure 5A&D, Supplementary Figure 6B) or 60μg/mouse anti-CD200R3 (Ba103) (Figure 4E), 300μg /mouse anti–Ly-6C (Monts 1, rat IgG2a) mAbs, or corresponding rat IgG2b or IgG2a isotype control mAbs were injected intravenously 24 hours before challenge. Note that the NIMP-R14 antibody clone is specific to the Ly-6G antigen (Supplementary Figure 4A-C). 300μL /mouse PBS- or clodronate-liposomes were injected intravenously either 24 hours before challenge, or both 24 and 48 hours before challenge. Specificity of cell depletion was evaluated in the blood, spleen and peritoneal lavage of naive 1543 mice 24 hours after NIMP-R14 (Supplementary Figure 4C-E) or Ba103 (Supplementary Figure 5). Please refer to "*Specificity and efficiency of cell depletion strategies" in the Supplemental Methods for more information.*

PAF-R antagonists ABT-491 (25μg/mouse) or CV-6209 (66μg/mouse) in 0.9% NaCl were injected intravenously 15min or 10min prior to challenge, respectively. H1-receptor antagonists cetirizine DiHCl, pyrilamine maleate , or triprolidine HCl at 300μg/mouse in 0.9% NaCl were injected intraperitoneally 30 minutes before challenge.

217

218 *Please refer to Supplemental Methods for details on: Generation of knock-in mice,*
219 *Antibodies and reagents, Flow cytometry, Specificity and efficiency of cell depletion*
220 *strategies, Statistics.*

221

RESULTS

Creation of VG1505 (mFcγRIIB$^{-/-}$ mFcγRIII$^{-/-}$ mFcγRIV$^{-/-}$) and VG1543 (mFcγRIIB$^{-/-}$ mFcγRIII$^{-/-}$ mFcγRIV$^{-/-}$ hFcγRIIA^{KI} hFcγRIIB^{KI} hFcγRIIIA^{KI} hFcγRIIIB^{KI}) mice

To delete the mouse low-affinity Fc receptors, a large targeting vector (BACvec)[31, 32] was constructed (as described in supplemental methods) to delete 106 kb of mouse genomic sequence encompassing the mouse Fcgr2b, Fcgr3, and Fcgr4 genes, and used to target VGF1 ES cells[33]. The low-affinity FcγR deleted allele (deletion of 1:170,956,770-171,063,353 from Chr1_H3 based on the mouse GRCh38 assembly) was given the designation VG1505 (Figure 1A).

To insert human FCGR3A and FCGR2A genes, a BACvec containing 69 kb of the corresponding human sequence flanked by long mouse homology arms was generated (refer to Supplemental Methods) and used to retarget VG1505 ES cells[31]. The subsequent allele in which the three mouse low affinity Fc receptors were replaced with hFCGR3A and hFCGR2A was given the designation VG1528 (Figure 1B). To insert human FCGR2B, FCGR2C and FCGR3B genes next to the human FCGR3A and FCGR2A genes, a BACvec was constructed containing an additional 142 kb of human sequence between a human homology arm, homologous to the end of the human insert in VG1528, and a mouse homology arm. This BACvec was used to retarget VG1528 ES cells, and resulted in an allele designated VG1543[31, 32] (insertion of human sequence from 1:161,500,441-161,679,348 on Chr1_q23.3 based on the human GRCh38 assembly) in which all five human low-affinity FcγR receptor genes replace the three mouse low-affinity FcγR genes (Figure 1C). The inserted human low-affinity FcγRs are in the same order as in the human genome and the human intergenic sequences are

retained intact. The human BAC sequences used encode for the polymorphic variants hFcγRIIA(H_{131}), hFcγRIIB(I_{232}), hFcγRIIC($Stop_{13}$), hFcγRIIIA(V_{158}) and hFcγRIIIB(NA2); therefore no expression of hFcγRIIC is expected in VG1543 mice.

VG1543 mice exhibit hFcγR expression patterns on immune cells comparable to that of humans

First, we determined that VG1505 and VG1543 mice exhibit normal immune cell composition (Supplementary Table 4). VG1505 mice demonstrate slightly elevated frequencies of granulocytes and monocytes in the blood and spleen, and macrophages in the peritoneum compared to VG1543 (Supplementary Figure 1A-C). Furthermore, VG1505 and VG1543 mice exhibit comparable mFcεRI and mFcγRI expression (Supplementary Figure 1D-F).

To compare the expression pattern of hFcγRs in VG1543 mice to that of humans, specific antibody staining and flow cytometry analysis was performed on cells isolated either from the blood of healthy human donors, or from the blood, spleen, lymph nodes, bone marrow, peritoneum and broncho-alveolar lavage (BAL) of VG1543 mice. All myeloid cells examined, including monocytes, macrophages, eosinophils, basophils and mast cells, and among lymphocytes B and NK cells, but not T cells, expressed at least one hFcγR (Figure 2A-B).

We detected hFcγRIIA (CD32A) staining on neutrophils, monocytes, eosinophils and platelets from the blood of healthy human donors (Figure 2A) as expected[26], and from the blood, spleen, lymph nodes, bone marrow, peritoneum and broncho-alveolar lavage of VG1543 mice (Figure 2B). VG1543 peritoneal mast cells also expressed hFcγRIIA. Like human blood basophils, VG1543 blood basophils expressed variably hFcγRIIA (Figure 2A-B), but not basophils from the spleen or bone

marrow; the low level of expression of hFcγRIIA on VG1543 blood basophils is in the range of expression found on basophils from human donors (Figure 2C). As expected, lymphocytes, including B, T and NK cells, did not express hFcγRIIA in humans and VG1543 mice (Figure 2A-B); notably we observed some background staining for hFcγRIIA on human B cells, as published previously[28]. Thus the hFcγRIIA expression pattern and level is comparable between VG1543 mice and blood from normal human donors.

In human blood hFcγRIIB was detected at high levels on all B cells and basophils, at lower levels variably on a proportion of monocytes (2-38% positive; n=4 donors), whereas other cells were mostly negative, *i.e.* neutrophils, eosinophils, NK cells, T cells, platelets (Figure 2A and Supplemental Figure 1A), as expected[34, 35]. Similarly, VG1543 mice expressed high levels of hFcγRIIB on B cells from blood, spleen, lymph node and peritoneum (Figure 2B). Furthermore, we observed variation in hFcγRIIB staining among B cell subpopulations isolated from the bone marrow and the peritoneum of VG1543 mice (Supplementary Figure 1B-C). VG1543 mice demonstrated robust hFcγRIIB expression on monocyte populations in the blood and lymphoid organs, yet no staining was observed on Ly6C^{hi} monocytes from the bone marrow. Only a fraction of donors we analysed demonstrated hFcγRIIB expression on blood monocytes (Supplemental Figure 2A), consistent with its previously reported variable expression on CD14^{lo} monocytes and absence of expression on CD14^{hi} monocytes[36]. Thus VG1543 exhibit over-expression of hFcγRIIB on blood monocytes compared to human blood monocytes. Interestingly, hFcγRIIB staining was higher on Ly6C^{low} "patrolling" monocytes than on Ly6C^{hi} "classical" monocytes from VG1543 mice (Supplemental Figure 2D), as it is on the analogous populations in human blood, CD14^{low}CD16^{hi} "patrolling" monocytes and CD14^{hi} "classical" monocytes (Supplemental Figure 2E).

297 Furthermore, spleen monocytes in human[36] and VG1543 mice express significant levels
298 of hFcγRIIB, reconciling hFcγRIIB expression on monocytes in this compartment
299 between human donors and VG1543 mice. Macrophages from the peritoneum, but not
300 from BAL, of VG1543 mice were found positive for hFcγRIIB (Figure 2B). Although
301 human basophils express high levels of hFcγRIIB[37], basophils from VG1543 mice were
302 negative (Figure 2A-B). Overall, VG1543 mice appear to express hFcγRIIB at similar
303 levels on B cells, at the high end of the range on monocytes, but not on basophils,
304 compared to humans.

305 Human neutrophils, monocytes, eosinophils, NK cells and a small proportion of
306 basophils were labelled positive with an anti-CD16 antibody recognizing both
307 hFcγRIIIA and hFcγRIIIB (Figure 2A), in accordance with known hFcγRIIIA (NK cells,
308 monocytes/macrophages and eosinophils) and hFcγRIIIB expression (neutrophils and
309 some basophils)[35]. Similarly, in the blood and organs from VG1543 mice, neutrophils
310 stained at high levels, and monocyte/macrophages, NK cells and basophils at variable
311 levels with anti-CD16 (Figure 2B and Supplemental Figure 1). Eosinophils from
312 VG1543 mice did not show detectable CD16 labelling, in accordance with 25% of
313 human donors (Supplemental Figure 1F). Interestingly, CD16 was apparent on only 30-
314 45% of NKp46$^+$ NK cells from the spleen of VG1543 mice, compared to 85-98% of
315 CD56$^+$ NK cells from human blood. Overall, VG1543 mice appear to express
316 hFcγRIIIA and hFcγRIIIB at similar levels on neutrophils and NK cells, at higher levels
317 on blood monocytes, but not on eosinophils nor on blood basophils, respectively,
318 compared to humans.

319

320 **Induction and mechanism of active systemic anaphylaxis in VG1543 mice**

Among human low-affinity hFcγRs, the activating IgG receptors hFcγRIIA and hFcγRIIIA, and the inhibitory IgG receptor hFcγRIIB, can bind mouse IgG isotypes[26, 28, 35] (Table 1): we therefore explored the capacity of these receptors to mediate active systemic anaphylaxis (ASA) triggered by i.v. BSA challenge in VG1505 and VG1543 mice immunised with BSA (Supplemental Figure 3). Following challenge, VG1543 mice, but not in VG1505 mice, suffered from a severe drop in body temperature and 50-100% mortality within 30 minutes (Figure 3A). Pre-treatment of VG1543 mice with blocking antibodies against activating hFcγRIIA (mAb IV.3)[28] abolished hypothermia and mortality (Figure 3B). hFcγRIIA is expressed by neutrophils, monocyte/macrophages, eosinophils, basophils and mast cells in VG1543 mice. Of these, neutrophils, monocyte/macrophages and basophils have been reported to contribute to IgG-PSA in mice[17-19]. Neutrophil depletion using either anti-Ly6G or anti-Gr1 mAbs protected VG1543 mice from ASA, but neither monocyte/macrophage nor basophil depletion (Figure 3C; Supplemental Figure 5B-E). Finally, PAF-receptor blockade protected from ASA-associated death and hypothermia, while H1-receptor antagonist cetirizine had no effect (Figure 3D, Supplemental Figure 5F-G). Altogether these data, obtained in this model of ASA contingent on hFcγR binding of mouse IgGs, demonstrate that VG1543 mice present with anaphylactic symptoms and a fatal reaction dependent on hFcγRIIA, neutrophils and PAF. They also demonstrate that mouse FcγRI, which is still expressed in both VG1505 mice and VG1543 mice, cannot induce anaphylaxis.

Aggregated human IVIG triggers passive systemic anaphylaxis in VG1543 mice

Although interactions between mouse IgG isotypes and some human FcγRs can result in the induction of anaphylactic reactions (Figure 3, Table 1 and [19, 27, 28]), such

346 models are far from recapitulating the variety of human IgG interactions with both
347 activating and inhibitory hFcγRs[38]. We therefore investigated whether anaphylaxis
348 could be initiated by triggering human FcγRs in VG1543 mice using aggregated human
349 intravenous immunoglobulin (IVIG) as a surrogate for human IgG-immune complexes.
350 Intravenous injection of 1mg heat-aggregated IVIG induced passive systemic
351 anaphylaxis (IVIG-PSA) in VG1543 mice, manifested by visual signs and severe
352 hypothermia, with a maximum temperature loss of 6-8°C 30-40 min after injection. This
353 reaction was dependant on the expression of hFcγR, since VG1505 mice were resistant
354 (Figure 4A). A dose response of heat-aggregated IVIG demonstrated that hypothermia
355 reaches a maximum at 1 mg, was lower at 500 or 300 µg, and was not observed at 30 µg
356 (Figure 4B & Supplemental Figure 4). A dose of 1mg was therefore chosen for all
357 subsequent IVIG-PSA, as it consistently induced in VG1543 mice a shock at sufficient
358 magnitude to assess the effect of receptor, cell and mediator blockade.
359
360 **hFcγRIIA and neutrophils contribute to IVIG-PSA in VG1543 mice**
361 hFcγRIIA blockade protected against both anaphylactic symptoms and
362 hypothermia during IVIG-PSA in VG1543 mice, (Figure 4C), even though VG1543
363 mice express also hFcγRIIIA and hFcγRIIIB that may induce cell activation[26, 35, 39].
364 Monocyte/macrophage depletion by toxic liposome administration had no effect (Figure
365 4D), whereas basophil depletion modestly reduced IVIG-PSA in VG1543 mice (Figure
366 4E). Neutrophil depletion, however, was protective (Figure 4F). Appropriate antibody-
367 mediated cell depletion was confirmed by flow cytometry analysis (Supplemental
368 Figure 4 and 5A), and we have previously demonstrated efficient monocyte/macrophage
369 depletion in the blood and spleen following liposome injection (Beutier et al 2016).
370 hFcγRIIB blockade, even using high doses of blocking mAb, did not modulate

anaphylactic symptoms in VG1543 mice induced by optimal (1mg; not shown) or suboptimal (250μg; Figure 4G) doses of heat-aggregated IVIG. Thus VG1543 mice are susceptible to PSA induced by human IgG, and the reaction proceeds primarily through neutrophils and the activating receptor hFcγRIIA, with a minor contribution of basophils, but does not require monocyte/macrophages, and is not negatively regulated by inhibitory hFcγRIIB.

Changes in hFcγR expression on myeloid cells following anaphylaxis

It has been proposed that changes in Fc receptor expression may be used as a biological marker for anaphylaxis, or an indicator of different pathways of activation[40]. We therefore investigated changes in hFcγR expression on circulating myeloid cell populations following IVIG-PSA in VG1543 mice. One hour after anaphylaxis induction, staining for activating hFcγR receptors was substantially reduced on neutrophils (Figure 5A), $Ly6C^{hi}$ (Figure 5B) and $Ly6C^{low}$ monocytes (Figure 5C) in the blood of VG1543 mice; entailing almost complete loss of hFcγRIIA on neutrophils and monocytes, and significant downregulation of hFcγRIII on neutrophils and $Ly6C^{low}$ monocytes. The inhibitory receptor hFcγRIIB was also significantly reduced on $Ly6C^{hi}$ monocytes, yet unchanged on $Ly6C^{low}$ monocytes and neutrophils. These changes in receptor staining were not due merely to increased quantities of circulating IgG, as the injection of non-aggregated IVIG did not affect receptor expression (Figure 5A-C). Receptor detection by anti-hFcγR mAbs may be influenced by pre-bound human IgG-immune complexes; however we confirmed that this was not the case using a panel of different antibodies with different recognition sites, both within and outside of the ligand-binding region. Furthermore, hIgG could be detected at low amounts on the surface of VG1543 neutrophils and monocytes isolated after IVIG-PSA (Supplementary

Figure 7 and Supplementary Methods), yet the limited amount of bound hIgG that we observe after PSA, particularly on neutrophils, certainly does not account for the several logs of reduction in receptor staining intensity. These data indicate active engagement of hFcγR on neutrophils and monocytes during IVIG-PSA, and suggest that these cells are each involved in responding to IgG-immune complexes, even though, in the case of monocytes, they may not be required for the induction of anaphylactic symptoms in VG1543 mice.

PAF and histamine contribute to IVIG-PSA in VG1543 mice

We assessed the contribution of the mediators PAF and histamine to IVIG-PSA in VG1543 mice, using receptor antagonists administered before PSA induction. PAF receptor blockade using two different antagonists (ABT-491 and CV-6209) significantly reduced the hypothermia associated with IVIG-PSA in VG1543 mice (Figure 6A-B). Cetirizine, Pyrilamine and Tropolidine are different histamine-receptor 1 antagonists that inhibit IgE-induced PSA to various extents (Supplemental Figure 8A-C). Cetirizine had no effect on IVIG PSA in VG1543 mice, unless combined with PAF-R antagonist ABT-491 (Supplemental Figures 8D-E). Pyrilamine and Tropolidine, however, significantly reduced the hypothermia associated with IVIG-PSA in VG1543 mice (Figure 6C-D). Of note, PAF-R antagonist ABT-491 injected at higher doses did not confer greater protection (Supplemental Figure 8F). Therefore both PAF and histamine contribute to IVIG-PSA, in agreement with the contribution of neutrophils and basophils, in knock-in mice expressing human low-affinity IgG receptors.

DISCUSSION

We demonstrate here that VG1543 mice, which exhibit genuine expression of all human low-affinity FcγRs, are susceptible to IgG-dependant anaphylaxis. VG1543, but not VG1505, mice experienced severe hypothermia following transfer of aggregated human IgG or following immunisation and challenge with the same antigen. These data show for the first time that, in a cognate context of activating and inhibitory human FcγR signalling, immune complexes formed by either mouse or human IgG can trigger cell activation, mediator release, and severe anaphylaxis.

Several transgenic mouse models have been developed previously to investigate the *in vivo* functions of human FcγRs (reviewed in [14, 35]). Transgenic approaches have their inherent flaws, however, in terms of reproducibility of human FcγR expression, heterogeneity of transgene expression between individuals of the same genotype, and instability between generations, as a result of random transgene integration into the genome. hFcγRIIA$(R_{131})^{tg}$ mice[41], hFcγRIIB$(I_{232})^{tg}$ [42], hFcγRIIIA$(F_{158})^{tg}$ and hFcγRIIIB^{tg} (unknown polymorphic variant)[43] mice each employ their respective genuine human promoter to drive transgene expression. Of these, it appears that only hFcγRIIA$(R_{131})^{tg}$ mice recapitulate the corresponding human expression patterns[28, 41], whereas hFcγRIIB$(I_{232})^{tg}$ mice exhibit abnormally high expression on circulating monocytes and granulocytes, and hFcγRIIIA$(F_{158})^{tg}$ hFcγRIIIB^{tg} mice have aberrant expression on DCs and eosinophils[29, 42]. Furthermore, the study of hFcγR-transgenic strains necessitates genetic backgrounds lacking endogenous mFcγRs, because mouse and human FcγRs cross-bind human and mouse IgG, respectively (Table 1). hFcγR-transgenic mice have been studied on a background deficient in the FcR γ-chain

444 signalling subunit ($FcR\gamma^{KO}$), that lacks functional expression of mFcγRI, mFcγRIII,
445 mFcγRIV and mFcεRI[44]. Unfortunately $FcR\gamma^{KO}$ mice have deficiencies in signalling
446 through several non-FcR molecules, including integrin, cytokine and growth factor
447 receptors, affecting leukocyte recruitment and vascular haemostasis; and these mice
448 maintain inhibitory mFcγRIIB expression that can modulate hFcγR-induced signalling[35,
449 45-47]. A $mFc\gamma R^{null}$ background, lacking all mouse IgG receptor expression but
450 maintaining FcR γ-chain expression, is a preferable approach, as exemplified in the
451 generation of $hFc\gamma RI^{tg}IIA^{tg}IIB^{tg}IIIA^{tg}IIIB^{tg}$ $mFc\gamma R^{null}$ mice by intercrossing of the five
452 single hFcγR-transgenic strains described above[29].
453
454 To circumvent the inherent issues of randomly integrated transgenics, we
455 employed gene knock–in technology to generate a mouse model deficient for the low-
456 affinity mouse IgG receptor locus ($mFc\gamma RIIB/III/IV^{KO}$; VG1505), and to insert the
457 human low-affinity IgG receptor locus in its stead ($hFc\gamma RIIA(H_{131})$-$hFc\gamma RIIB(I_{232})$-
458 $hFc\gamma RIIC(Stop_{13})$-$hFc\gamma RIIIA(V_{158})$-$hFc\gamma RIIIB(NA2)^{KI}$; VG1543). Consequently,
459 VG1543 mice demonstrate hFcγR expression consistent with that observed in humans[26,
460 35], with some minor differences: eosinophils lack hFcγRIIIA expression and basophils
461 lack hFcγRIIB expression. In addition, hFcγRIIIA and hFcγRIIB expression is higher
462 on blood monocytes compared to humans; nevertheless hFcγRIIB on these cells in
463 VG1543 remains very much closer to that observed in humans, when compared to the
464 expression reported in $hFc\gamma RI^{tg}IIA^{tg}IIB^{tg}IIIA^{tg}IIIB^{tg}$ $mFc\gamma R^{null}$ mice[29]. Of note, VG1543
465 represent the first mouse model of $hFc\gamma RIIA(H_{131})$ and $hFc\gamma RIIIA(V_{158})$ expression,
466 which is particularly advantageous for the study of human IgG2. Indeed $hFc\gamma RIIA(H_{131})$
467 binds significantly better human IgG2 than the polymorphic variant $hFc\gamma RIIA(R_{131})$,
468 which is expressed in hFcγRIIA transgenic animals[38, 48]; and $hFc\gamma RIIIA(V_{158})$ binds

469 human IgG2 whereas polymorphic variant hFcγRIIIA(F_{158}), expressed in hFcγRIIIA^{tg}
470 mice, does not[38, 43, 48].

471 Here we identify for the first time that, within the context of native co-
472 expression with other activating and inhibitory hFcγRs, hFcγRIIA drives IgG-
473 anaphylaxis induction. hFcγRIIA blockade indeed protected VG1543 mice against
474 systemic anaphylaxis induced by aggregated human IVIG. The transfer of IVIG
475 aggregated *ex vivo* mimics the formation of polyclonal hIgG immune complexes *in vivo*,
476 since the subclass composition reflects that of human serum: 63% IgG1, 29% IgG2, 5%
477 IgG3 and 3% IgG4. All human FcγRs expressed in VG1543 mice bind human IgG1 and
478 IgG3, only hFcγRIIA(H_{131}) and hFcγRIIIA(V_{158}) bind human IgG2, and all except
479 hFcγRIIIB(NA2) bind human IgG4. Yet hFcγRIIA(H_{131}) binds IgG2 with >7-fold
480 higher affinity than hFcγRIIIA(V_{158})[38], and therefore the IgG2 component of aggregated
481 IVIG may bias towards hFcγRIIA(H_{131}) engagement over the other hFcγRs expressed in
482 VG1543 mice. hFcγRIIA blockade also protected VG1543 mice from systemic
483 anaphylaxis and death following immunisation and challenge with the same antigen.
484 This is a less physiological model, as it relies on human hFcγRs cross-binding mouse
485 IgGs. Among the activating receptors expressed in VG1543 mice, only hFcγRIIA binds
486 mouse IgG1 (Table 1) - the predominant IgG isotype produced during ASA
487 immunisation - and logically therefore predominantly contributes to anaphylaxis
488 induction.

489 While the protective effect of hFcγRIIA blockade in IVIG-PSA suggests that
490 hFcγRIIIA and hFcγRIIIB are not individually capable of triggering systemic
491 anaphylaxis, we cannot formally exclude a cooperative role of these receptors in
492 anaphylaxis induction via hFcγRIIA in VG1543 mice. Indeed, we could not efficiently

493 block hFcγRIIIA and/or hFcγRIIIB *in vivo* using available anti-hFcγRIII antibodies
494 (data not shown). We did observe significant hFcγRIIIA/B down-regulation on
495 circulating neutrophils and monocytes after IVIG-PSA, but not after injection of non-
496 aggregated IVIG (Figure 6), supporting the notion that these receptors are actively
497 engaging with IgG immune complexes, despite not triggering a systemic reaction.
498 Indeed, in models of autoantibody-induced inflammation, hFcγRIIA and hFcγRIIIB
499 expressed on neutrophils were found to individually and cooperatively promote immune
500 complex-induced reactions; however hFcγRIIA alone promoted associated injury and
501 inflammation, whereas hFcγRIIIB rather mediated homeostatic clearance of immune
502 complexes[39, 49], suggesting that hFcγRIIA, but not hFcγRIIIB, is able to induce
503 detrimental reactions *in vivo*. Anaphylaxis induced by aggregated IVIG was also
504 demonstrated in the hFcγRI^{tg}IIA^{tg}IIB^{tg}IIIA^{tg}IIIB^{tg} mFcγR^{null} mouse model[29], but the
505 contributing hFcγRs were not identified.
506
507 Importantly, VG1505 and VG1543 mice still express the high-affinity mouse
508 receptor mFcγRI, which is expressed on monocytes, tissue resident monocyte-derived
509 cells and specific macrophage populations[26, 50, 51] (Supplementary Figure 1). Even so,
510 VG1505 mice were resistant to IVIG-PSA (and active anaphylaxis) induction,
511 demonstrating that mFcγRI alone cannot trigger anaphylaxis, and that anaphylactic
512 reactions in VG1543 mice rely exclusively on hFcγR triggering. We previously reported
513 that the human counterpart of mFcγRI, hFcγRI (CD64) was sufficient to induce
514 systemic anaphylaxis in transgenic mice lacking mouse FcγRs[27]. We used for this
515 former study the only reported hFcγRI-transgenic mouse: it expresses this receptor on
516 monocytes and macrophages as in humans, but also constitutively on neutrophils,
517 contrarily to humans[35, 52]. Anaphylaxis in these mice relied on both neutrophils and

518 monocytes/macrophages[27]. Human FcγRI is not expressed in the VG1543 background,
519 and the question remains open whether hFcγRI can participate in IgG-induced
520 anaphylaxis in a context of native hFcγR expression. We have developed a novel
521 hFcγRI knock-in mouse strain that does not present the discrepant expression of
522 existing hFcγRI-transgenic models[29, 52]: hFcγRI is expressed on monocytes,
523 macrophages and dendritic cells, but not constitutively on neutrophils (data not shown).
524 We are currently crossing this mouse strain to VG1543 mice, to create a fully hFcγR-
525 humanized knock-in mouse model, which should enable us in the future to address the
526 relative contribution of hFcγRI in a model recapitulating all hFcγR expression.
527
528 Anaphylaxis is driven by the release of anaphylactogenic mediators from
529 myeloid cells[4, 53]. The contribution of any given cell population is therefore determined
530 by the requisite expression of activating FcγR, the capacity of the cells to release active
531 mediators, and a cells' potential for negative inhibition of FcγR signalling by expression
532 of inhibitory FcγRIIB[54]. In wild-type (wt) mice, pathways of active systemic
533 anaphylaxis and passive IgG anaphylaxis rely predominantly on monocyte and/or
534 neutrophil activation via mFcγRIII, with a minor contribution of mFcγRIV, and
535 subsequent PAF release[18, 19, 55]. Considering genetic evolution, the functional homolog
536 of mFcγRIII is hFcγRIIA, and that of mFcγRIV is hFcγRIIIA (H. Watier, personal
537 communication)[35]. It is therefore consistent that hFcγRIIA, which exhibits prominent
538 expression on all circulating myeloid cells, like mFcγRIII, may be the predominant IgG
539 receptor contributing to anaphylaxis in VG1543 mice. We previously demonstrated that
540 transgenic expression of hFcγRIIA(R_{131}) was sufficient to induce passive active
541 systemic anaphylaxis, and that IgG-induced PSA in hFcγRIIA(R_{131})^{tg} mFcγRI/IIB/III^{KO}
542 mice required monocytes and neutrophils[28].

Here, we identify that neutrophils are mandatory for anaphylaxis in VG1543 mice, whereas we could not identify a contribution for monocytes/macrophages, although they express hFcγRIIA. This discrepancy between mouse models may be due to expression of inhibitory hFcγRIIB, absent in hFcγRIIA(R_{131})^{tg} mFcγRI/IIB/III^{KO} mice, but elevated on VG1543 blood monocytes compared to humans. Blood monocytes express consistently hFcγRIIB in VG1543 mice but we and others have identified variable hFcγRIIB on monocytes, particularly CD14^{lo} blood monocytes, and prominent expression on only a fraction of human donors[36] (Supplementary Figure 2). Spleen monocytes, however, significantly express hFcγRIIB in humans[36] and VG1543 mice. Indeed, hFcγRIIB binds to all subclasses of human IgG[38] and therefore may inhibit monocyte activation following engagement by IVIG aggregates in VG1543 mice. On one hand, we observed down-regulation of inhibitory hFcγRIIB on circulating Ly6C^{hi} and Ly6C^{low} monocytes following IVIG-PSA suggesting its engagement by IVIG-immune complexes and potential inhibitory signalling by this receptor; on the other hand blockade of hFcγRIIB did not modulate anaphylactic symptoms in VG1543 mice. hFcγRIIB, and the inhibitory signals it can induce, do not appear to regulate this model of anaphylaxis. These data do not favour a contribution of monocytes to anaphylaxis in VG1543 mice. We cannot, however, exclude a potential contribution of blood monocytes (mostly hFcγRIIB negative) to human anaphylaxis.

The contribution of basophils to anaphylaxis models in mice remains controversial: mIgG1-induced PSA[17] and mIgG2a-induced PSA[55] were inhibited following antibody-mediated basophil depletion, but mIgG1-induced PSA was unaffected in Mcpt8-cre mice that exhibit >90% basophil deficiency[56]. In an active model of peanut-induced anaphylaxis, involving both IgE and IgG, both antibody- or

568 diphtheria toxin-mediated basophil depletion significantly reduced hypothermia[57].
569 Human basophils express variable levels of hFcγRIIA and high levels of hFcγRIIB, yet
570 could not be activated by hIgG immune complexes *in vitro*, suggesting that hFcγRIIB-
571 dependent negative regulation is dominant over hFcγRIIA-dependent basophil
572 activation[37]. VG1543 mice express hFcγRIIA at low levels on circulating basophils, but
573 within the range of that observed on peripheral blood cells from healthy donors (Figure
574 2A-B). Unlike human basophils, however, VG1543 basophils do not express hFcγRIIB:
575 that we do not identify a major contribution of basophils to anaphylaxis in VG1543
576 mice cannot be due to hFcγRIIB inhibition of hFcγRIIA-mediated signalling.

577 We reported previously that neutrophils predominantly contribute to ASA in wt
578 mice and that the transfer of human neutrophils can restore anaphylaxis in resistant
579 mice[13, 19]. Neutrophils were mandatory for IVIG-PSA (and ASA) in VG1543 mice,
580 since neutrophil depletion abolished hypothermia and protected from death. Both of
581 these anaphylaxis models were dependent on hFcγRIIA, which is expressed at very high
582 levels on both human and VG1543 mouse neutrophils, whereas inhibitory hFcγRIIB
583 expression is found only on a small subset of neutrophils. This low or absent hFcγRIIB
584 expression implies that, unlike monocytes, neutrophil activation is not, or marginally,
585 regulated by inhibitory hFcγRIIB. Neutrophils also contributed to hFcγRIIA-dependent
586 PSA in hFcγRIIA(R_{131})^{tg} mFcγRI/IIB/III^{KO} mice[28] in the absence of other hFcγR
587 expression. We demonstrate now that the contribution of neutrophils to IgG-induced
588 anaphylaxis is also predominant in the context of native hFcγR expression in VG1543
589 mice. Such an observation is of crucial consideration when we acknowledge that
590 neutrophils comprise >60% of circulating blood cells in humans.
591

Finally, we identified that the soluble mediator PAF was responsible for a significant proportion of IVIG-PSA-induced hypothermia (and ASA-associated death), a finding concurrent with a dominant pathway initiated by hFcγRIIA on neutrophils. Neutrophils are indeed the major producers of PAF in humans[58]. Among the three Histamine receptor antagonists tested, two (Pyrilamine and Tripolidine) significantly inhibited IVIG-induced anaphylaxis by themselves, and one (Cetirizine) only had an effect when combined with PAF-R antagonists. These findings suggest that both PAF and histamine contribute to hypothermia and mortality in the VG1543 model. These results are in agreement with the inefficacy of H1-antihistamine treatment alone on systemic anaphylactic symptoms in patients. Reports by Vadas and colleagues indicate a correlation between levels of circulating PAF, rather than histamine, with anaphylaxis severity[12], and identified PAF as a central mediator of human anaphylaxis pathogenesis[59]; which aligns with our findings reported herein using locus-swapped human low-affinity hFcγR^{KI} mice.

Our data indicate that IgG-dependant anaphylaxis in VG1543 mice proceeds via an activating pathway dependent on hFcγRIIA and neutrophils, with a contribution of basophils, and driven by the mediators PAF and histamine. Although expressed in this novel knock-in mouse model, hFcγRIIIA and hFcγRIIIB were not sufficient to trigger anaphylaxis. That such drastic anaphylaxis induction is possible in the context of native inhibitory and activating hFcγR expression suggests a similar pathway may occur in humans. VG1543 mice represent an attractive knock-in model for the study of human low-affinity IgG receptors, in which the encoding genes remain expressed in their cognate genetic environment, including intergenic sequences; and consequently cell surface expression largely reflects that of humans. Although the polymorphisms

617 expressed in the VG1543 mouse represent a section of individuals within the population,
618 other people express alternate and/or heterozygous polymorphisms, some of which have
619 been demonstrated to predispose to immunological susceptibility or resistance[14]. It
620 would be clinically relevant to extend studies in hFcγR-knock in mice to understand the
621 effect of hFcγR polymorphisms on cell activation and subsequent biological responses,
622 and therefore on sensitivity to anaphylaxis or other allergic diseases involving IgG
623 antibodies.
624

ACKNOWLEDGMENTS

We are thankful to O. Godon, B. Iannascoli and O. Richard-LeGoff for technical help, P. Vieira and L. Reber for scientific advice and D. Sinnaya for administrative help (Institut Pasteur, Paris). We are thankful to our colleagues for their generous gifts: R. Coffman (DNAX, Palo Alto, CA, USA), R. Good (USFCM, Tampa, FL, USA), H. Karasuyama (Tokyo Medical and Dental University Graduate School, Tokyo, Japan) and D. Voehringer (Universitätsklinikum, Erlangen, Germany) for antibodies. Cl2MDP was a gift of Roche Diagnostics GmbH. This work was supported by the European Research Council (ERC)–Seventh Frame-work Program (ERC-2013-CoG 616050); additional support by the Institut Pasteur and the Institut National de la Santé et de la Recherche Médicale (INSERM). C.G. was supported partly by a stipend from the Pasteur - Paris University (PPU) International PhD program and by the Institut Carnot Pasteur Maladies Infectieuses, and partly by the Balsan company. F.J. is an employee of the Centre National de La Recherche Scientifique (CNRS). H.B. is supported by a fellowship from the University Pierre et Marie Curie.

AUTHORSHIP AND CONFLICT OF INTEREST STATEMENTS

C.G. performed all experiments, with contributions from F.J., D.A.M. and H.B.; A.M., L.E.M. and N.T. designed mouse targeting and generated mouse strains; N.v.R. provided reagents; C.G., F.J., L.E.M. and P.B. analysed and discussed results; C.G. and P.B. wrote the manuscript; P.B. supervised and designed the research.

LM, NT and AM are employees of Regeneron Pharmaceuticals, Inc. and hold stock in the company. H.B., P.B, C.G., B.I., F.J. and D.A.M. declare no competing financial interests.

650 **FIGURE LEGENDS**

651

652 **Figure 1: Humanization of the mouse low-affinity receptor locus.** Representations
653 are not drawn to scale. (A) Deletion of mouse Fcgr2b, Fcgr4 and Fcgr3 genes in a single
654 targeting step, deleting mouse sequences from 1:170,956,770 to 1:171,063,353 on
655 mouse Chr1_H3 (based on mouse GRCh38). (B) Insertion of human FCGR3A and
656 FCGR2A genes and (C) insertion of FCGR2B, FCGR3B and FCGR2C genes. The total
657 human sequence inserted in VG1543 ranges from 1:161,500,441 to 1:161,679,348 on
658 human Chr1_q23.3, based on human GRCh38. Mouse genomic coordinates are in black,
659 human genomic coordinates are in grey, light grey block arrow indicates Hygromycin
660 selection cassettes, dark grey block arrows indicate Neomycin selection cassettes, black
661 triangles represent Loxp sites, empty triangles represent Frt sites and grey triangles
662 represent Lox2372 sites.

663

664 **Figure 2: Human FcγR expression on immune cell populations from VG1543 mice**
665 **recapitulates expression patterns in humans**
666 (A) hFcγRIIA, hFcγRIIB, hFcγRIIIA and hFcγRIIIB staining on immune cells from
667 human peripheral blood, assessed by fluorescent antibody labelling and flow cytometric
668 analysis. Shaded histograms indicate staining with an isotype control antibody,
669 excepting hFcγRIIB where shaded histograms indicate a fluorescence-minus-one
670 (FMO) control. (B) hFcγR staining on immune cells isolated from different tissues of
671 VG1543 mice, as indicated. Shaded histograms indicate background staining from
672 VG1505 mice. Data are representative of at least 2 independent experiments; total n>3.
673 BAL: bronchoalveolar lavage. Numbers indicate frequency of cells positive for FcγR

674 staining. (C) Individual variation in hFcγRIIA expression on basophils isolated from 4
675 different blood donors (upper panels) or from 4 different1543 mice (lower panels).
676
677 **Figure 3: VG1543 mice are susceptible to active systemic anaphylaxis, dominantly**
678 **mediated by hFcγRIIA, neutrophils and PAF.**
679 Indicated mice were immunised and challenged with BSA, and central temperatures and
680 survival rates were monitored. (A) Change in body temperature (upper panel) and
681 survival (lower panel) during BSA-ASA in VG1505 (crossed circles) and VG1543
682 (squares) mice. (B-D) BSA-ASA in VG1505 and VG1543 mice, and VG1543 mice
683 treated with (B) anti-hFcγRIIA blocking mAbs or isotype control, (C) anti-Ly6G mAbs
684 or isotype control, (D) vehicle (NaCl) or PAF-R antagonist ABT-491. Data are
685 represented as mean ± SEM and are representative of at least 2 independent experiments.
686 Numbers indicate mortality per experimental group; X represents 100% mortality. (#
687 $p<0.05$; ### $p<0.001$, Log-rank (Mantel-Cox) test for survival; * $p<0.05$, ** $p<0.01$,
688 Student's t-test of individual time points from 10 to 40min)
689
690 **Figure 4: Aggregated human IVIG triggers passive systemic anaphylaxis in**
691 **VG1543 mice, mediated by hFcγRIIA and neutrophils.**
692 VG1505 (circles) and VG1543 (squares) mice were injected with (A) 1mg or (B)
693 indicated amounts of heat-aggregated IVIG and central temperatures monitored. (C-F)
694 IVIG-PSA (1mg) in VG1543 mice injected with (C) anti-hFcγRIIA blocking mAbs, (D)
695 toxin-containing liposomes, (E) anti-CD200R3 mAbs, (F) anti-Ly6G mAbs, or
696 corresponding isotype or PBS controls, prior to anaphylaxis induction. (G) IVIG-PSA
697 (250μg) in VG1543 mice injected with indicated amounts of anti-hFcγRIIB blocking
698 mAbs. White or grey squares indicate treated mice; black squares indicate isotype or

vehicle controls. (A-F) Data are represented as mean ± SEM and are representative of at least 2 independent experiments. (G) Data are represented as mean values of independent experiments. (*p<0.05, **p<0.01; 2-way RM-ANOVA).

Figure 5: Reduction in hFcγR expression on circulating myeloid cell populations after IVIG-PSA. hFcγRIIA, hFcγRIIB and hFcγRIII expression on (A) blood neutrophils, (B) $Ly6C^{hi}$ and (C) $Ly6C^{low}$ monocytes from VG1543 mice; 1 hour after injection of vehicle (NaCl), non-aggregated IVIG (non-agg) or heat aggregated-IVIG and PSA induction (HA-IVIG). Background staining on cells from VG1505 mice is shown 1 hour after injection of heat aggregated-IVIG. Values represent ΔGeoMean between specific staining and corresponding isotype or FMO control, pooled from three independent experiments. Representative histograms are shown in (D); background staining of isotype control is indicated by shaded histograms; VG1505 mice by grey histograms. (***p<0.001, *p<0.05, unpaired t test with Welch's correction)

Figure 6: The anaphylactic mediators PAF and histamine are responsible for IVIG-PSA in VG1543 mice. PSA was induced by 1mg heat-aggregated IVIG and central temperatures monitored: indicated mice were pre-treated,with PAF-R antagonists (A) ABT-491 or (B) CV-6209, H1-R antagonists (C) pyrilamine maleate or (D) triprolidine hydrochloride, or with vehicle (NaCl). Data are represented as mean ± SEM and are representative of at least 2 independent experiments (*p<0.05, **p<0.01, VG1543 treated vs controls, 2-way RM-ANOVA)

TABLES

Table 1: Binding and crossbinding of human and mouse IgG subclasses to human and mouse FcγRs

-, no binding; +/-, very-low binding; +, low-binding; ++, medium binding; +++, high binding. Adapted from data reported in [19, 38, 60, 61] and unpublished data.

		HUMAN				MOUSE			
		IgG1	**IgG2**	**IgG3**	**IgG4**	**IgG1**	**IgG2a/c**	**IgG2b**	**IgG3**
HUMAN	**hFcγRI**	+++	-	+++	+++	-	+++	+++	+/-
	hFcγRIIA(H131)	++	+	+	+	+	+	+	-
	hFcγRIIA(R131)	++	+	+	+	++	+	+	-
	hFcγRIIB	+	+/-	+	+	-	-	+/-	-
	hFcγRIIC	+	+/-	+	+	-	-	+/-	-
	hFcγRIIIA(V158)	+	+/-	+++	+	-	+/-	-	-
	hFcγRIIIA(F158)	+	+/-	++	+	-	-	-	-
	hFcγRIIIB(NA1)	+	-	++	-	-	-	-	-
	hFcγRIIIB(NA2)	+	-	++	-	-	-	-	-
	hFcγRIIIB(SH)	+	-	++	-	-	-	-	-
MOUSE	**mFcγRI**	+++	-	++	++	-	+++	+	+/-
	mFcγRIIB	-	+/-	-	-	++	+	++	-
	mFcγRIII	++	++	+/-	-	+	+	+	-
	mFcγRIV	++	+	++	+/-	-	+++	+++	-

SUPPLEMENTAL FIGURE LEGENDS

Supplemental Figure 1: VG1505 and VG1543 mice demonstrate normal immune cell composition of major compartments, and comparable expression of mFcεRI mFcγRI.

(A) Spleens taken from VG1505 mice and VG1543 mice were comparable in size. (B) Leukocyte counts in total blood were enumerated using an automatic blood cell analyser and (C; see also supplementary table 4) frequency of blood immune cell populations was determined by flow cytometry. (D) mFcεRI expression on peritoneal mast cells from VG1505 mice and VG1543 mice: representative histograms are shown and values represent ΔGeoMean between specific staining and isotype control. (E) Anti-IgE staining on basophils in the blood, spleen and bone marrow, as a surrogate measure of mFcεRI expression. (F) Representative histograms showing mFcγRI expression on various monocyte and macrophage populations isolated from VG1505 mice and VG1543 mice.

Supplemental Figure 2: Variability in hFcγR expression on monocytes and eosinophils from different human blood donors. B cells and monocytes exhibit subpopulation-distinct variation in hFcγR expression.

Cells were isolated from the (A, E, F) blood of healthy human donors, or (B) bone marrow, (C) peritoneum, or (D) blood of VG1543 mice, for flow cytometry analysis. (A) Variable expression hFcγRIIB on monocytes from the blood of 4 different human donors; numbers indicate frequency of cells positive for FcγR staining. (B, C) Representative histograms showing hFcγRIIB expression on VG1543 B cell subpopulations: (B) mature B cells ($B220^{hi}$ $CD43^{neg}$ IgM^{+} IgD^{+}) and ($B220^{low}$ $CD43^{neg}$)

immature (IgM^{+}), pro (IgM^{neg}) and pre ($IgM^{neg}IgD^{neg}$) B cells from the bone marrow, and (C) peritoneal B1a cells (IgM^{+} $CD11b^{+}$ IgD^{low}) and B2 cells (IgM^{+} $CD11b^{neg}$ IgD^{hi}). Numbers indicate ΔGeoMean between specific staining and FMO controls. Data is representative of at least 2 independent experiments, n>3. (D, E) Discrimination of classical vs patrolling monocyte subsets in the blood of VG1543 mice (D) or human donors (E); differential hFcγRIIA**,** hFcγRIIB and hFcγRIII expression on monocyte subsets is shown by representative histograms. Shaded grey histograms indicate background staining from VG1505 mice; shaded blue histograms indicate background staining with an isotype control antibody (hFcγRIIA, hFcγRIII**)**, or an FMO control (hFcγRIIB). (F) Variable expression of hFcγRIII on eosinophils from the blood of 4 different human donors

Supplemental Figure 3: Immunisation with BSA in CFA/IFA induces BSA-specific IgG1 and IgG2 in VG1505 and VG1543 mice. (A) Anti-IgG1 and (B) anti-IgG2a/b/c BSA-specific ELISA results from two independent experiments are represented as serial dilution curves of individual mouse sera, and as average curve (insets). VG1505 (dashed black line) and VG1543 (solid black line) mice exhibit comparable antibody titres; excl** (blue line) indicates mice that were excluded from challenge due to low antibody titres; positive (pos: red line) and negative (neg: dotted black line) ELISA controls are indicated.

Supplemental Figure 4: Antibody clone NIMP-R14 specifically targets Ly-6G antigen and efficiently depletes neutrophils *in vivo.*

(A-C) Blood sampled from naive mice (pool of n=4) was stained with FITC-conjugated NIMP-R14 in combination with fluorescent antibody clones 1A8 (anti-Ly-6G; A), RB6-8C5 (anti-GR1: binds Ly-6C and Ly-6G; B), or anti-Ly-6C (Monts 1; C) with or without pre-blocking with an excess of unconjugated NIMP-R14 or 1A8. Staining was assessed by flow cytometry, and representative plots are shown pre-gated on single, live $CD11b^{+}$ cells. (D-F) VG1543 mice were treated with 300µg NIMP-R14 or rat isotype control antibody (rIgG2b) and blood and tissues were sampled 24 hours later and frequencies of specific cell populations determined by flow cytometry: gating strategies are shown and frequencies of neutrophils and monocyte/macrophages in the (D) blood, (E) spleen and (F) peritoneum; and percentage of basophils in the (G) blood and (H) spleen, and (I) mast cells in the peritoneum. (D-F) Data is pooled from 2 independent experiments.

Supplemental Figure 5: Basophils, monocyte/macrophages and histamine were not found to contribute to BSA-ASA in VG1543 mice. (A) VG1543 mice were treated with 30µg anti-CD200R3 (Ba103) or rat isotype control antibody (rIgG2b) and blood and tissues sampled 24 hours later: representative gating strategy and percentage of basophils in the blood and spleen; and percentage of mast cells in the peritoneum. (B-G) Change in body temperature and survival during BSA-ASA in VG1505 and VG1543 mice, and VG1543 mice treated with (B) anti-GR1 mAbs, (C&E) toxic liposomes, (D) anti-CD200R3 mAbs, (F) H1-receptor antagonist Cetirizine, (G) PAF-R antagonist ABT-491, or respective controls. Data are represented as mean ± SEM and are representative of at least 2 independent experiments. (E) BSA-ASA with high mortality in VG1543 mice treated with PBS or toxin-containing liposomes before challenge:

repeat of panel 5C. (G) BSA-ASA with no mortality in VG1543 mice treated or not with PAF-R antagonist before challenge: repeat of Figure 3D.

Supplemental Figure 6: PSA-induced hypothermia of VG1543 mice after injection of high-dose heat-aggregated IVIG, or basophil depletion (A) VG1543 mice were injected with indicated amounts of heat-aggregated IVIG and central temperatures monitored. Data are represented as individual replicates of each dose. (B) VG1543 mice treated with 30μg anti-CD200R3 (Ba103) or isotype control 24 hours before injection of 1mg heat aggregated IVIG and PSA induction.

Supplemental Figure 7: Observed reduction in hFcγR expression on circulating myeloid cell populations after IVIG-PSA is not due to binding inhibition by surface bound hIgG. hFcγR expression on blood (A) neutrophils, (B) Ly6C^{hi} and (C) Ly6C^{low} monocytes from VG1543 mice 1 hour after injection of non-aggregated IVIG (non-agg) or heat aggregated-IVIG (HA-IVIG, leading to PSA). Only non-blocking antibodies were used for detecting hFcgR expression, to avoid competition with ligand (*i.e.* IVIG) binding: anti-CD32 clone FLI8.26 defines hFcγRIIA+B expression, anti-CD32(R131) clone 3D3 defines hFcγRIIB expression, and anti-CD16 clone MEM-154 defines hFcγRIIIA+B expression. Background staining on cells from VG1505 mice is shown 1 hour after injection of heat aggregated-IVIG. Values represent GeoMean of specific staining, pooled from three independent experiments. (***$p<0.001$, **$p<0.01$, Student's t test). (D) Staining of surface hIgG bound *ex vivo* by incubating blood neutrophils and monocytes isolated from (left histograms) naïve VG1543 mice or (central histograms) PAF-injected VG1543 mice (0.3μg PAF injected i.v. to induce PAF-dependent anaphylaxis) with HA-IVIG (20μg/mL). These histograms were

compared to histograms (right) representing staining of surface hIgG bound *in vivo* to blood cell populations, isolated 1 hour after IVIG-PSA. Representative histograms are shown from 2-3 independent experiments, n≥3. Shaded histograms represent labelling with secondary antibody alone (left and central panels) or FMO control (right panels).

Supplemental Figure 8: Role of mediators in PSA. (A-C) Antihistamine treatment inhibits IgE-PSA: VG1505 mice were sensitised by transfer of anti-TNP specific IgE and challenged with TNP-BSA. Indicated mice were injected i.p. with H1 receptor antagonists (A) cetirizine 300μg or (B) pyrilamine 300μg 30min prior, or (C) triprolidine 200μg 20min prior to challenge. *NB* triprolidine was injected at 200μg/mouse in (C): this dose was increased to 300μg for IVIG-PSA pretreatment (Figure 6D). (D-E) VG1543 were treated (D) with cetirizine alone or (E) in combination with PAF-R antagonist ABT-491 prior to IVIG-PSA. Data is (D) representative or (E) collated from 6 independent experiments. ***$p<0.001$, VG1543 controls vs VG1543 + PAF-R antagonist and VG1543 controls vs VG1543 + PAF-R antagonist + antihistamine, ** $p<0.05$ VG1543 + PAF-R antagonist vs VG1543 + PAF-R antagonist + antihistamine, Student's t-test at 30min. (F) Administration of PAF-R antagonist ABT-491 at an increased dose does not confer increased protection from IVIG-PSA: VG1543 were injected i.v. with 25 or 100μg of PAF-R antagonist ABT-491 15 min before the induction of IVIG-PSA.

REFERENCES

1. Mullins RJ, Dear KB, Tang ML. Time trends in Australian hospital anaphylaxis admissions in 1998-1999 to 2011-2012. J Allergy Clin Immunol 2015; 136:367-75.
2. Nocerino R, Leone L, Cosenza L, Berni Canani R. Increasing rate of hospitalizations for food-induced anaphylaxis in Italian children: An analysis of the Italian Ministry of Health database. J Allergy Clin Immunol 2015; 135:833-5 e3.
3. Turner PJ, Gowland MH, Sharma V, Ierodiakonou D, Harper N, Garcez T, et al. Increase in anaphylaxis-related hospitalizations but no increase in fatalities: an analysis of United Kingdom national anaphylaxis data, 1992-2012. J Allergy Clin Immunol 2015; 135:956-63 e1.
4. Lee JK, Vadas P. Anaphylaxis: mechanisms and management. Clin Exp Allergy 2011; 41:923-38.
5. Fisher MM, Baldo BA. Mast cell tryptase in anaesthetic anaphylactoid reactions. Br J Anaesth 1998; 80:26-9.
6. Cheifetz A, Smedley M, Martin S, Reiter M, Leone G, Mayer L, et al. The incidence and management of infusion reactions to infliximab: a large center experience. Am J Gastroenterol 2003; 98:1315-24.
7. Dybendal T, Guttormsen AB, Elsayed S, Askeland B, Harboe T, Florvaag E. Screening for mast cell tryptase and serum IgE antibodies in 18 patients with anaphylactic shock during general anaesthesia. Acta Anaesthesiol Scand 2003; 47:1211-8.
8. Golden DB. Patterns of anaphylaxis: acute and late phase features of allergic reactions. Novartis Found Symp 2004; 257:101-10; discussion 10-5, 57-60, 276-85.
9. Mertes PM, Alla F, Trechot P, Auroy Y, Jougla E. Anaphylaxis during anesthesia in France: an 8-year national survey. J Allergy Clin Immunol 2011; 128:366-73.
10. Laroche D, Gomis P, Gallimidi E, Malinovsky JM, Mertes PM. Diagnostic value of histamine and tryptase concentrations in severe anaphylaxis with shock or cardiac arrest during anesthesia. Anesthesiology 2014; 121:272-9.
11. Vadas P, Gold M, Perelman B, Liss GM, Lack G, Blyth T, et al. Platelet-activating factor, PAF acetylhydrolase, and severe anaphylaxis. N Engl J Med 2008; 358:28-35.
12. Vadas P, Perelman B, Liss G. Platelet-activating factor, histamine, and tryptase levels in human anaphylaxis. J Allergy Clin Immunol 2013; 131:144-9.
13. Jonsson F, Mancardi DA, Albanesi M, Bruhns P. Neutrophils in local and systemic antibody-dependent inflammatory and anaphylactic reactions. J Leukoc Biol 2013; 94:643-56.
14. Gillis C, Gouel-Cheron A, Jonsson F, Bruhns P. Contribution of Human FcgammaRs to Disease with Evidence from Human Polymorphisms and Transgenic Animal Studies. Front Immunol 2014; 5:254.
15. Oettgen HC, Martin TR, Wynshaw-Boris A, Deng C, Drazen JM, Leder P. Active anaphylaxis in IgE-deficient mice. Nature 1994; 370:367-70.
16. Miyajima I, Dombrowicz D, Martin TR, Ravetch JV, Kinet JP, Galli SJ. Systemic anaphylaxis in the mouse can be mediated largely through IgG1 and Fc gammaRIII. Assessment of the cardiopulmonary changes, mast cell

900 degranulation, and death associated with active or IgE- or IgG1-dependent
901 passive anaphylaxis. J Clin Invest 1997; 99:901-14.
902 17. Tsujimura Y, Obata K, Mukai K, Shindou H, Yoshida M, Nishikado H, et al.
903 Basophils play a pivotal role in immunoglobulin-G-mediated but not
904 immunoglobulin-E-mediated systemic anaphylaxis. Immunity 2008; 28:581-9.
905 18. Strait RT, Morris SC, Yang M, Qu XW, Finkelman FD. Pathways of
906 anaphylaxis in the mouse. J Allergy Clin Immunol 2002; 109:658-68.
907 19. Jönsson F, Mancardi DA, Kita Y, Karasuyama H, Iannascoli B, Van Rooijen N,
908 et al. Mouse and human neutrophils induce anaphylaxis. J Clin Invest 2011;
909 121:1484-96.
910 20. Iff ET, Vaz NM. Mechanisms of anaphylaxis in the mouse. Similarity of shock
911 induced by anaphylaxis and by mixtures of histamine and serotonin. Int Arch
912 Allergy Appl Immunol 1966; 30:313-22.
913 21. Million M, Fioramonti J, Zajac JM, Bueno L. Effects of neuropeptide FF on
914 intestinal motility and temperature changes induced by endotoxin and platelet-
915 activating factor. Eur J Pharmacol 1997; 334:67-73.
916 22. van de Veen W, Stanic B, Yaman G, Wawrzyniak M, Sollner S, Akdis DG, et al.
917 IgG4 production is confined to human IL-10-producing regulatory B cells that
918 suppress antigen-specific immune responses. J Allergy Clin Immunol 2013;
919 131:1204-12.
920 23. Rispens T, Derksen NI, Commins SP, Platts-Mills TA, Aalberse RC. IgE
921 production to alpha-gal is accompanied by elevated levels of specific IgG1
922 antibodies and low amounts of IgE to blood group B. PLoS One 2013; 8:e55566.
923 24. Patil SU, Ogunniyi AO, Calatroni A, Tadigotla VR, Ruiter B, Ma A, et al.
924 Peanut oral immunotherapy transiently expands circulating Ara h 2-specific B
925 cells with a homologous repertoire in unrelated subjects. J Allergy Clin
926 Immunol 2015; 136:125-34 e12.
927 25. Hoh RA, Joshi SA, Liu Y, Wang C, Roskin KM, Lee JY, et al. Single B-cell
928 deconvolution of peanut-specific antibody responses in allergic patients. J
929 Allergy Clin Immunol 2015.
930 26. Bruhns P. Properties of mouse and human IgG receptors and their contribution
931 to disease models. Blood 2012; 119:5640-9.
932 27. Mancardi DA, Albanesi M, Jonsson F, Iannascoli B, Van Rooijen N, Kang X, et
933 al. The high-affinity human IgG receptor FcgammaRI (CD64) promotes IgG-
934 mediated inflammation, anaphylaxis, and antitumor immunotherapy. Blood
935 2013; 121:1563-73.
936 28. Jönsson F, Mancardi DA, Zhao W, Kita Y, Iannascoli B, Khun H, et al. Human
937 FcgammaRIIA induces anaphylactic and allergic reactions. Blood 2012;
938 119:2533-44.
939 29. Smith P, DiLillo DJ, Bournazos S, Li F, Ravetch JV. Mouse model
940 recapitulating human Fcgamma receptor structural and functional diversity. Proc
941 Natl Acad Sci U S A 2012; 109:6181-6.
942 30. Meyer T, Robles-Carrillo L, Davila M, Brodie M, Desai H, Rivera-Amaya M, et
943 al. CD32a antibodies induce thrombocytopenia and type II hypersensitivity
944 reactions in FCGR2A mice. Blood 2015; 126:2230-8.
945 31. Valenzuela DM, Murphy AJ, Frendewey D, Gale NW, Economides AN,
946 Auerbach W, et al. High-throughput engineering of the mouse genome coupled
947 with high-resolution expression analysis. Nat Biotechnol 2003; 21:652-9.

32. Macdonald LE, Karow M, Stevens S, Auerbach W, Poueymirou WT, Yasenchak J, et al. Precise and in situ genetic humanization of 6 Mb of mouse immunoglobulin genes. Proc Natl Acad Sci U S A 2014; 111:5147-52.
33. Auerbach W, Dunmore JH, Fairchild-Huntress V, Fang Q, Auerbach AB, Huszar D, et al. Establishment and chimera analysis of 129/SvEv- and C57BL/6-derived mouse embryonic stem cell lines. Biotechniques 2000; 29:1024-8, 30, 32.
34. Veri MC, Gorlatov S, Li H, Burke S, Johnson S, Stavenhagen J, et al. Monoclonal antibodies capable of discriminating the human inhibitory Fcgamma-receptor IIB (CD32B) from the activating Fcgamma-receptor IIA (CD32A): biochemical, biological and functional characterization. Immunology 2007; 121:392-404.
35. Bruhns P, Jonsson F. Mouse and human FcR effector functions. Immunol Rev 2015; 268:25-51.
36. Tutt AL, James S, Laversin SA, Tipton TR, Ashton-Key M, French RR, et al. Development and Characterization of Monoclonal Antibodies Specific for Mouse and Human Fcgamma Receptors. J Immunol 2015; 195:5503-16.
37. Cassard L, Jonsson F, Arnaud S, Daeron M. Fcgamma receptors inhibit mouse and human basophil activation. J Immunol 2012; 189:2995-3006.
38. Bruhns P, Iannascoli B, England P, Mancardi DA, Fernandez N, Jorieux S, et al. Specificity and affinity of human Fc{gamma} receptors and their polymorphic variants for human IgG subclasses. Blood 2009; 113:3716-25.
39. Tsuboi N, Asano K, Lauterbach M, Mayadas TN. Human neutrophil Fcgamma receptors initiate and play specialized nonredundant roles in antibody-mediated inflammatory diseases. Immunity 2008; 28:833-46.
40. Khodoun MV, Strait R, Armstrong L, Yanase N, Finkelman FD. Identification of markers that distinguish IgE- from IgG-mediated anaphylaxis. Proc Natl Acad Sci U S A 2011; 108:12413-8.
41. McKenzie SE, Taylor SM, Malladi P, Yuhan H, Cassel DL, Chien P, et al. The role of the human Fc receptor Fc gamma RIIA in the immune clearance of platelets: a transgenic mouse model. J Immunol 1999; 162:4311-8.
42. Li F, Ravetch JV. Inhibitory Fcgamma receptor engagement drives adjuvant and anti-tumor activities of agonistic CD40 antibodies. Science 2011; 333:1030-4.
43. Li M, Wirthmueller U, Ravetch JV. Reconstitution of human Fc gamma RIII cell type specificity in transgenic mice. J Exp Med 1996; 183:1259-63.
44. Takai T, Li M, Sylvestre D, Clynes R, Ravetch JV. FcR gamma chain deletion results in pleiotrophic effector cell defects. Cell 1994; 76:519-29.
45. Borges L, Cosman D. LIRs/ILTs/MIRs, inhibitory and stimulatory Ig-superfamily receptors expressed in myeloid and lymphoid cells. Cytokine Growth Factor Rev 2000; 11:209-17.
46. Zarbock A, Abram CL, Hundt M, Altman A, Lowell CA, Ley K. PSGL-1 engagement by E-selectin signals through Src kinase Fgr and ITAM adapters DAP12 and FcR gamma to induce slow leukocyte rolling. J Exp Med 2008; 205:2339-47.
47. Boulaftali Y, Hess PR, Kahn ML, Bergmeier W. Platelet immunoreceptor tyrosine-based activation motif (ITAM) signaling and vascular integrity. Circ Res 2014; 114:1174-84.
48. Warmerdam PA, van de Winkel JG, Gosselin EJ, Capel PJ. Molecular basis for a polymorphism of human Fc gamma receptor II (CD32). J Exp Med 1990; 172:19-25.

49. Chen K, Nishi H, Travers R, Tsuboi N, Martinod K, Wagner DD, et al. Endocytosis of soluble immune complexes leads to their clearance by FcgammaRIIIB but induces neutrophil extracellular traps via FcgammaRIIA in vivo. Blood 2012; 120:4421-31.
50. Mancardi DA, Jonsson F, Iannascoli B, Khun H, Van Rooijen N, Huerre M, et al. The murine high-affinity IgG receptor Fc(gamma)RIV is sufficient for autoantibody-induced arthritis. J Immunol 2011; 186:1899-903.
51. Langlet C, Tamoutounour S, Henri S, Luche H, Ardouin L, Gregoire C, et al. CD64 Expression Distinguishes Monocyte-Derived and Conventional Dendritic Cells and Reveals Their Distinct Role during Intramuscular Immunization. J Immunol 2012; 188:1751-60.
52. Heijnen IA, van Vugt MJ, Fanger NA, Graziano RF, de Wit TP, Hofhuis FM, et al. Antigen targeting to myeloid-specific human Fc gamma RI/CD64 triggers enhanced antibody responses in transgenic mice. J Clin Invest 1996; 97:331-8.
53. Brown SG, Stone SF, Fatovich DM, Burrows SA, Holdgate A, Celenza A, et al. Anaphylaxis: Clinical patterns, mediator release, and severity. J Allergy Clin Immunol 2013.
54. Smith KG, Clatworthy MR. FcgammaRIIB in autoimmunity and infection: evolutionary and therapeutic implications. Nat Rev Immunol 2010; 10:328-43.
55. Khodoun MV, Kucuk ZY, Strait RT, Krishnamurthy D, Janek K, Clay CD, et al. Rapid desensitization of mice with anti-FcgammaRIIb/FcgammaRIII mAb safely prevents IgG-mediated anaphylaxis. J Allergy Clin Immunol 2013; 132:1375-87.
56. Ohnmacht C, Schwartz C, Panzer M, Schiedewitz I, Naumann R, Voehringer D. Basophils orchestrate chronic allergic dermatitis and protective immunity against helminths. Immunity 2010; 33:364-74.
57. Reber LL, Marichal T, Mukai K, Kita Y, Tokuoka SM, Roers A, et al. Selective ablation of mast cells or basophils reduces peanut-induced anaphylaxis in mice. J Allergy Clin Immunol 2013; 132:881-8 e11.
58. Jouvin-Marche E, Ninio E, Beaurain G, Tence M, Niaudet P, Benveniste J. Biosynthesis of Paf-acether (platelet-activating factor). VII. Precursors of Paf-acether and acetyl-transferase activity in human leukocytes. J Immunol 1984; 133:892-8.
59. Gill P, Jindal NL, Jagdis A, Vadas P. Platelets in the immune response: Revisiting platelet-activating factor in anaphylaxis. J Allergy Clin Immunol 2015; 135:1424-32.
60. Nimmerjahn F, Bruhns P, Horiuchi K, Ravetch JV. Fc gamma RIV: a novel FcR with distinct IgG subclass specificity. Immunity 2005; 23:41-51.
61. Mancardi DA, Iannascoli B, Hoos S, England P, Daeron M, Bruhns P. FcgammaRIV is a mouse IgE receptor that resembles macrophage FcepsilonRI in humans and promotes IgE-induced lung inflammation. J Clin Invest 2008; 118:3738-50.

SUPPLEMENTAL METHODS

Generation of mFcγRIIB, mFcγRIII and mFcγRIV knock-out mice.

A targeting construct (Figure 1A) for deleting the mouse Fcgr2b, Fcgr3 and FcgR4 genes (encoding mFcγRIIB, mFcγRIII, and mFcγRIV respectively) in a single targeting step was constructed by using *VELOCIGENE* technology[1]. Mouse sequences were obtained from bacterial artificial chromosome (BAC) clone RP23-395F6. A donor fragment was constructed by cloning a lox'd neomycin cassette flanked by site-specific recombination sites. More specifically, 5′ mouse homology arm, corresponding to 270bp of mouse sequence located 3796 bp downstream of Fcgr2b, was PCR'ed using oligos (Supplemental Tables 1 and 2) and cloned upstream of a mutant lox'd neomycin selection cassette followed by a mouse 3′ homology arm corresponding to 342 bp of mouse sequence (PCR using oligos noted in Supplemental Tables 1 and 2) located 4001 bp upstream of the ATG of Fcgr3. This donor fragment was inserted into Escherichia coli strain DH10B containing the mouse BAC clone RP23-395F6 and a recombination enzyme vector. Cells were grown in drug selection medium. Upon homologous recombination (BHR) at the locus, a drug selection cassette replaces the Fcgr2b, Fcgr3 and Fcgr4 genes. Individual clones were grown, and the targeted BAC DNA that contains a lox'd drug cassette in place of the Fcgr2b, Fcgr3 and Fcgr4 genes was extracted. Targeted cells were identified by PCR using up detect primer set and down detect primer set (Supplemental Tables 1 and 2). Part of the vector was sequenced to confirm proper mouse-cassette junctions and pulsed field gel electrophoresis was used to establish insert size and expected restriction fragment length.

The targeting vector (LTVEC) VG1505 was linearized and used to electroporate VGF1 mouse embryonic stem (ES) cells. Upon homologous recombination at the locus 106kb of the endogenous Fcgr2b, Fcgr3 and Fcgr4 locus is thereby deleted & replaced by lox'd

neomycin cassette resulting in an ES cell that does not express endogenous Fcgr2b, Fcgr3 and Fcgr4 genes. Correctly targeted ES cells were introduced into an eight cell stage mouse embryo by the *VELOCIMOUSE* method[2]. *VELOCIMICE* (F0 mice fully derived from the donor ES cell) bearing the deleted Fcgr2b, Fcgr3 and Fcgr4 genes were identified by genotyping for loss of mouse allele using a modification of allele assay (Supplemental Table 3).

Generation of knock-in hFcγRIIA(H_{131})-hFcγRIIB(I_{232})-hFcγRIIC($Stop_{13}$)-hFcγRIIIA(V_{158})-hFcγRIIIB(NA2) mice

Targeting constructs (Figure 1B-C) for subsequent humanization of mouse mFcγRs by two sequential targeting steps, were constructed by using *VELOCIGENE* technology[1]. For the first targeting construct, VG1528, human sequences were obtained from bacterial artificial chromosome (BAC) clone CTD-2514J12. BACvec VG1528 was constructed in four steps as described in Supplemental Tables 1 and 2. In step 1, a donor fragment was constructed by cloning a frt'd hygromycin cassette flanked by site-specific recombination sites. More specifically, 5′ BAC backbone homology arm, corresponding to 384bp of pBeloBAC11, was PCR'ed using oligos (Supplemental Table 1) and cloned upstream of a frt'd hygromycin selection cassette followed by a human 3′ homology arm corresponding to 342bp of human sequence (PCR'd using oligos in Supplemental Tables 1 and 2) located 19kb upstream of the human FCGR3A gene (encoding hFcγRIIIA). BHR with this donor fragment deleted 41kb from the 5' end of CTD-2514J12, replacing it with an I-CeuI site and the frt'd hygromycin cassette to make VI209. In step 2, VI209 was modified by BHR to insert a PI-SceI site and spec cassette at the 3' end to make VI212 (Supplemental Tables 1 and 2). In step 3, RP23-395F6 was modified by BHR to delete the entire 106kb mouse low-affinity mFcγR locus (Fcgr2b, Fcgr3 and Fcgr4 genes), replacing it with a lox'd neomycin cassette flanked by a 5'

I-CeuI site and a 3' PI-SceI site. The extra PI-SceI site in the backbone was then deleted by AscI digestion and ligation to make VI208. In step 4, the 69kb human hFcγRs-encoding fragment from VI212 was ligated into the I-CeuI and PI-SceI sites of VI208, replacing the lox'd neomycin cassette to make the final LTVEC VG1528.

For the second targeting construct VG1543, human sequences were obtained from bacterial artificial chromosome (BAC) clone RP11-697E5. BACvec VG1543 was constructed in three steps as described in Supplemental Tables 1 and 2. In step 1, a donor fragment was constructed by cloning a spectinomycin cassette flanked by site-specific recombination sites. More specifically, 5′ homology arm, corresponding to 59bp of human sequence and BAC backbone sequence that is 4558 bp downstream of FCGR3A, was ligated to a spectinomycin selection cassette followed by a 3′ homology arm corresponding to 333bp of backbone sequence in pBACe3.6. BHR with this donor fragment trimmed the human hFcγR locus on the proximal end of RP11-697E5, deleting the PI-SceI site, to make VI217. In step 2, VI217 was modified by BHR using a donor fragment consisting of 5' homology arm corresponding to 258bp of BAC backbone sequence in pBACe3.6, a frt'd hygromycin cassette flanked by a 5' NotI site and a 3' PI-SceI site, and 3' homology arm corresponding to 274bp of human sequence 1188bp upstream of FCGR2B to make VI222. In step 3, the 47kb mouse distal homology arm with lox'd neomycin cassette from VI208 was ligated into the NotI and PI-SceI sites of VI222, replacing the frt'd hygromycin cassette to make the final LTVEC VG1543.

The targeting vectors were linearized and used to electroporate mouse embryonic stem (ES) cells [3]. Upon homologous recombination at the locus 106kb of the endogenous mouse low-affinity FcγR locus (Fcgr2b, Fcgr3 and Fcgr4 genes) is thereby deleted & replaced by human FCGR2B, FCGR3B, FCGR2C, FCGR3A and FCGR2A genes (encoding hFcγRIIB variant I_{232}, hFcγRIIIB variant NA2, hFcγRIIC variant $stop_{13}$, hFcγRIIIA variant V_{158}, and

hFcγRIIA variant H_{131}) by sequential targeting of VG1528 and VG1543, resulting in an ES cell that expresses low-affinity human hFcγR genes instead of endogenous low-affinity mouse mFcγR genes. Correctly targeted ES cells were introduced into an eight cell stage mouse embryo by the *VELOCIMOUSE* method [2]. *VELOCIMICE* (F0 mice fully derived from the donor ES cell) bearing the human FCGR2B, FCGR3B, FCGR2C, FCGR3A and FCGR2A genes were identified by genotyping for loss of mouse allele & gain of human allele using a modification of allele assay (Supplemental Table 3).

Antibodies and reagents

Bovine serum albumin (BSA), complete and incomplete Freund's adjuvant (CFA, IFA) and ABT-491 were from Sigma-Aldrich; Cetirizine DiHCl was from Selleck Chemicals; TNP-BSA was from Santa Cruz. Fluorescently labelled anti-mouse CD11b, CD43, CD49b, CD115, CD335 (NKp46), Ly6C, Ly6G, Gr-1, B220, IgD and SiglecF were from BD Biosciences; anti-mouse CD19 and IgM from Biolegend; and anti-mouse IgE from eBioscience. Fluorescently labelled anti-human CD3, CD11b, CD14, CD15, CD19, CD56 were from Miltenyi Biotec; anti-human CD61 and CD16 (3G8) from BD Biosciences; anti-hFcγRIIA (IV.3) from Stem Cell Technologies. Fluorescently labelled anti-hFcγRIIB (2B6) in a chimeric mouse-human IgG1 $N_{297}A$ form was prepared in-house.

PBS-liposomes and Clodronate-liposomes were prepared as published[4]. The hybridoma producing mAbs anti-hFcγRIIA (IV.3) was provided by C.L. Anderson (Heart & Lung Research Institute, Columbus, OH, USA), anti-Gr1 (RB6-8C4) by R. Coffman (DNAX Research Institute, Palo Alto, California,USA), and anti–Ly-6G (NIMP-R14) by C. Leclerc (Institut Pasteur, Paris, France). mAbs were purified from hybridoma supernatants by Protein G-affinity purification. Purified mAbs anti-Ba103 were provided by H. Karasuyama (Tokyo Medical and Dental University Graduate School, Tokyo, Japan).

Tissue processing

Cells were isolated from the blood and organs of VG1505 and VG1543 mice as follows. Spleens were dissociated through a 70µm cell strainer into MACS buffer (PBS /0.5%BSA /2mM EDTA) and RBC lysis was performed using an ammonium chloride-based buffer. For isolation of skin cells, ears were split into dorsal and ventral halves and roughly chopped before digestion with 0.25mg/mL Liberase TL ResearchGrade (Roche) + 0.1mg/mL DNase (Sigma) for 1h at 37°C (800rpm; Eppendorf Thermomixer), washed with 10x volume of PBS/ 10%FBS /2mM EDTA and processed through a 100µm cell strainer. Livers were perfused with cold PBS before dissection, and processed using the GentleMACS liver dissociation kit and the Octo Dissociator (Miltenyi Biotec). Cells were isolated from the peritoneum by lavage with 6mL cold PBS; BALs were performed 3x with 1mL PBS. For blood leukocyte analysis, a precise volume of heparinised blood was subjected to RBC lysis and washed with MACS buffer.

Flow cytometry

Human EDTA-collected blood was obtained from the blood bank « Établissement Français du Sang ». After red blood cell lysis, leukocytes were stained with fluorescently labelled mAbs for 30min at 4°C. Human cell populations were distinguished as: $CD15^{+}CD193^{neg}$ neutrophils; $CD193^{+}CD15^{low}$ eosinophils; $CD3^{+}$ T cells; $CD19^{+}$ B cells; $CD56^{+}$ NK cells; $CD123^{+}CD203c^{low}Fc\varepsilon RI^{hi}$ basophils; $CD14^{+}$ monocytes; $CD14^{hi}CD16^{low}$ classical monocytes and $CD14^{low}CD16^{hi}$ patrolling monocytes; $CD61^{+}$ platelets.

Isolated single cell suspensions from mouse blood and organs were stained with fluorescently labelled mAbs for 30-40min at 4°C. Mouse cell populations were distinguished by FSC/SSC characteristics and by surface markers as follows: neutrophils ($CD11b^{+}$ $Ly6C^{low}$ $Ly6G^{+}$),

monocytes (classical $CD11b^{+}$ $Ly6G^{neg}$ $Ly6C^{hi}$ or patrolling $CD11b^{+}$ $Ly6G^{neg}$ $CD115^{+}$ $Ly6C^{low}$), peritoneal macrophages ($CD11b^{hi}$ $Gr1^{low}$), alveolar macrophages ($CD11c^{hi}$), liver and bone marrow macrophages ($CD11b^{hi}$ $Gr1^{low}F4/80^{+}$), eosinophils ($CD11b^{+}$ $SiglecF^{+}$ SSC^{hi}), basophils ($CD45^{low}$ $mIgE^{+}$ $CD49b^{+}$), mast cells ($mIgE^{+}CD49b^{+}CD117^{+}$), platelets ($CD41^{+}$), T cells ($CD3^{+}$; $CD4^{+}/CD8^{+}$), B cells ($CD19^{+}/B220^{+}$, subpopulations as in Supplemental Figure 1), and NK cells ($NKp46^{+}CD49b^{+}$).

hFcγRIIA was identified by the specific mAb clone IV.3. hFcγRIIB was identified by the clone 2B6[5], expressed as a chimeric mouse-human IgG1 $N_{297}A$ variant to inhibit unspecific binding via the Fc portion of the antibody. We used an anti-CD16 antibody (clone 3G8) to characterise jointly hFcγRIIIA and hFcγRIIIB expression, because we could not identify, using a series of commercially available anti-CD16 antibodies, an antibody able to distinguish surface expression of hFcγRIIIA(V_{158}) from hFcγRIIIB(NA2). In supplemental figure 7: anti-CD32 clone FLI8.26 defines hFcγRIIA+B expression; anti-CD32(R131) clone 3D3 defines hFcγRIIB expression only, because VG1543 mice express the H131 variant of hFcγRIIA; anti-CD16 clone MEM-154 defines hFcγRIIIA+B expression. mFcγRI was identified using the specific clone X54-5/7.1 (BD Biosciences).

For *ex vivo* binding of cells with human IgG, blood cell suspensions were incubated first with aggregated IVIG (20μg/mL) for 1 hour on ice, and then stained with a fluorescently labelled antibody cocktail, including anti-human IgG Fab-specific goat $F(ab')_2$ fragment (Jackson Immunoresearch). Cells isolated from VG1543 mice after IVIG-PSA were stained with the secondary antibody alone.

Samples were run on a MACSQuant flow cytometer (Miltenyi) and data analysed using FlowJo Software (Treestar Inc.).

Specificity and efficiency of cell depletion strategies:

Appropriate antibody-mediated cell depletion using anti-Ly6G (NIMP-R14) and anti-CD200R3 (Ba103) was examined by flow cytometry analysis. NIMP-R14 treatment (300μg) efficiently depleted neutrophils in the blood, spleen and peritoneum. The percentage of total $CD11b^{+}CD115^{+}$ monocytes in the blood and $CD11b^{+}Gr1^{int}$ monocytes in the spleen were unaffected, while the percentage of $CD11b^{+}F4/80^{+}$ macrophages in the peritoneum increased slightly. The percentage of blood basophils was slightly increased, but total numbers were unaffected and spleen basophils and peritoneal mast cells were not affected. We did, however observe that the frequency of $Ly6C^{hi}$ monocytes decreased while the frequency of $Ly6C^{low}$ monocytes increased following NIMP-R14 treatment, a phenomenon which may reflect epitope masking by NIMP-R14 due to a low-level cross-recognition. NIMP-R14 therefore efficiently depletes neutrophils with some effects on other cell populations. Ba103 administration at 30μg per mouse induced basophil depletion in the blood and spleen, without affecting circulating neutrophils and monocytes (data not shown), or peritoneal mast cells. Yet the depletion of basophils was incomplete (up to 70%), and not uniformly efficient across individuals (Supplementary Figure 5A). We therefore administered Ba103 at a two-fold greater dose (60μg/mouse). Although we could not detect a significant increase in depletion compared to the 30μg dose (data not shown), this increased dose indicated a minor contribution of basophils to anaphylaxis severity (Figure 4E).

We have previously demonstrated efficient monocyte/macrophage depletion in the blood and spleen following intravenous liposome injection (Beutier et al 2016. JACI *in press*); whereas peritoneal macrophages remained intact. In efforts to achieve complete monocyte/macrophage depletion, we combined multiple injections of clodronate liposomes with different routes of administration, resulting in higher total liposome load: these approaches were inconclusive, however, and while we were efficiently able to deplete resident macrophages, we observed

increases in numbers of circulating inflammatory monocytes, and wildly inconsistent responses during IVIG-PSA. Indeed, toxic liposomes can affect all phagocytic cell populations, and approaches to increase their efficacy also augment non-specific effects**.** For this study, we confirmed that the ability of macrophages to mediate thrombocytopenia (reflecting capacity to engage and engulf antibody-bound cells, and by logical extension, immune complexes) remains intact following antibody-mediated depletion strategies (*e.g.* NIMP-R14 or Ba103), but is blocked following intravenous clodronate liposome injection at the doses used herein.

Statistics

Statistical analyses were performed using Prism. Survival was analysed by a log-rank (Mantel-Cox) test to compare test subjects and controls. Temperature loss during ASA was compared using a Student's t-test of individual time points. Temperature loss during PSA was compared by 2-way repeated measures ANOVA (RM-ANOVA), except in Supplementary Figure 8E in which groups were compared using a Student's t-test at 30min. hFcγR expression in Figure 5 and Supplementary Figure 7 was compared using an unpaired t-test with Welch's correction for unequal variances.

Supplemental References

1. Valenzuela DM, Murphy AJ, Frendewey D, Gale NW, Economides AN, Auerbach W, et al. High-throughput engineering of the mouse genome coupled with high-resolution expression analysis. Nat Biotechnol 2003; 21:652-9.
2. Poueymirou WT, Auerbach W, Frendewey D, Hickey JF, Escaravage JM, Esau L, et al. F0 generation mice fully derived from gene-targeted embryonic stem cells allowing immediate phenotypic analyses. Nat Biotechnol 2007; 25:91-9.
3. Auerbach W, Dunmore JH, Fairchild-Huntress V, Fang Q, Auerbach AB, Huszar D, et al. Establishment and chimera analysis of 129/SvEv- and C57BL/6-derived mouse embryonic stem cell lines. Biotechniques 2000; 29:1024-8, 30, 32.
4. Van Rooijen N, Sanders A. Liposome mediated depletion of macrophages: mechanism of action, preparation of liposomes and applications. J Immunol Methods 1994; 174:83-93.
5. Veri MC, Gorlatov S, Li H, Burke S, Johnson S, Stavenhagen J, et al. Monoclonal antibodies capable of discriminating the human inhibitory Fcgamma-receptor IIB (CD32B) from the activating Fcgamma-receptor IIA (CD32A): biochemical, biological and functional characterization. Immunology 2007; 121:392-404.

Figure 1

A. Deletion of Fcgr2b, Fcgr4 and Fcgr3 genes (encoding mFcγRIIB, mFcγRIV and mFcγRIII)

B. Insertion of FCGR3A and FCGR2A, encoding hFcγRIIIA(V_{158}) and hFcγRIIA(H_{131})

C. Insertion of FCGR2B, FCGR3B and FCGR2C, encoding hFcγRIIB(I_{232}), hFcγRIIIB(NA2) and hFcγRIIC($stop_{13}$)

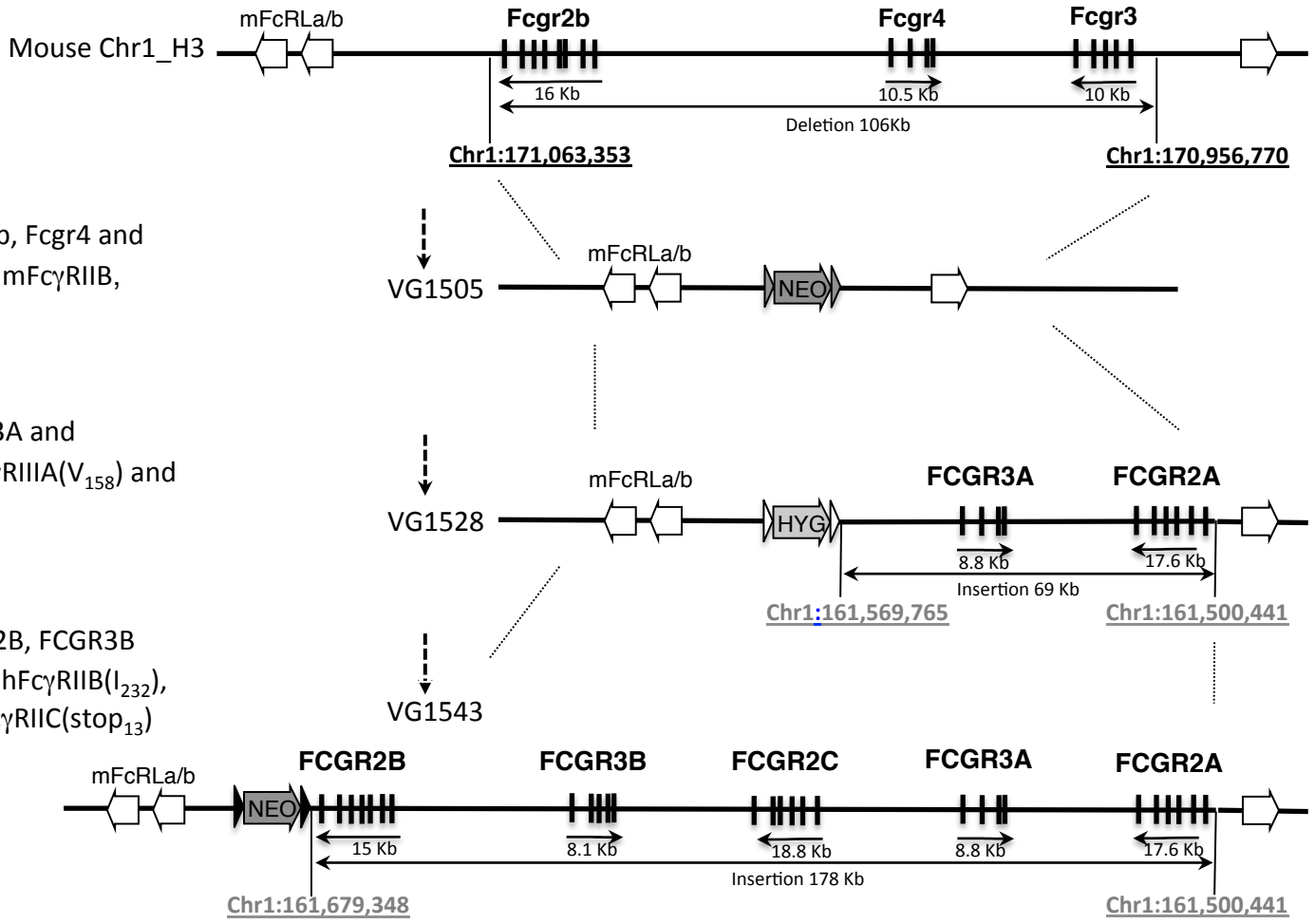

Figure 2

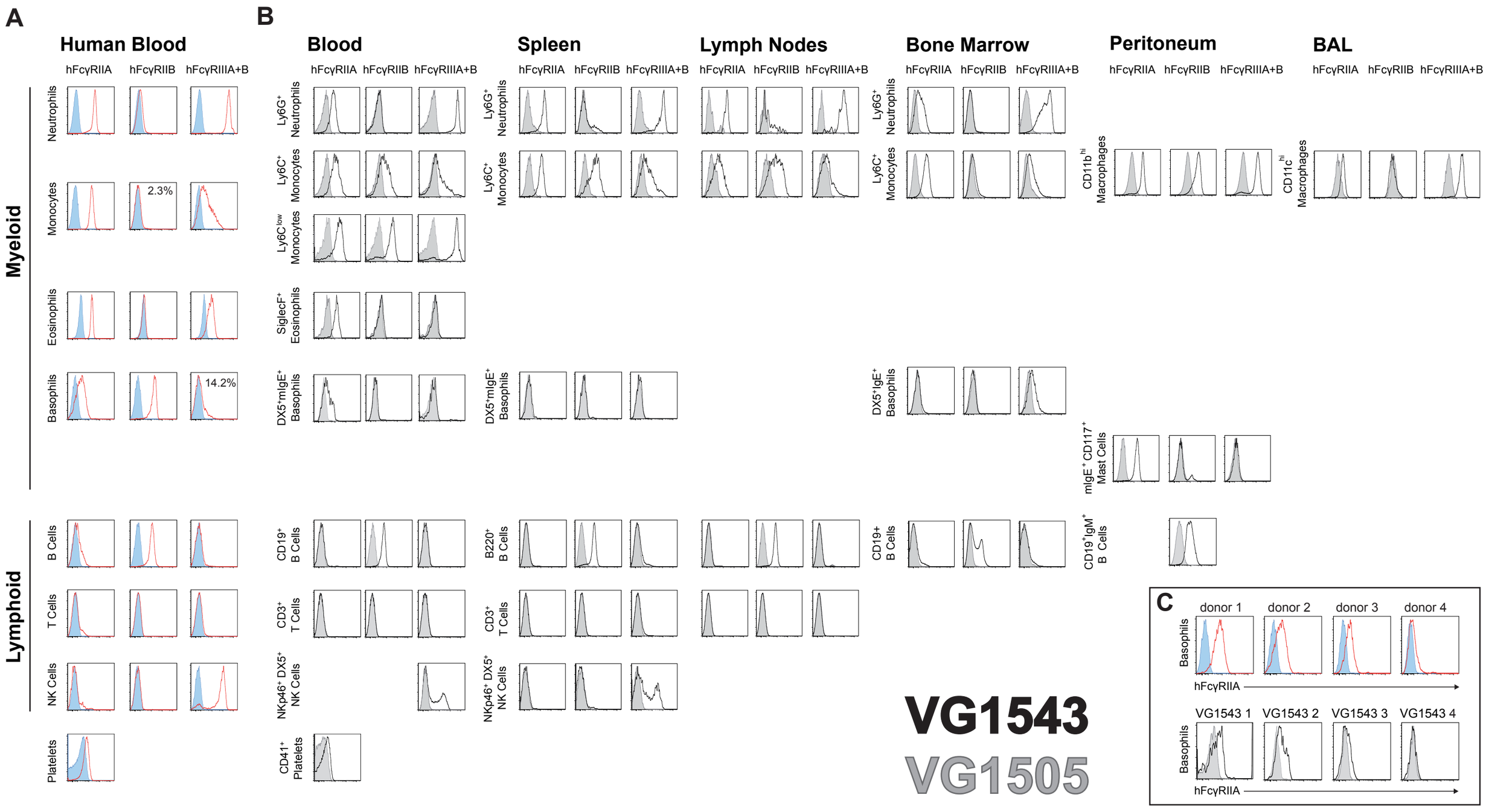
A
Human Blood
hFcγRIIA
hFcγRIIB
hFcγRIIIA+B
Myeloid
Neutrophils
Monocytes
2.3%
Eosinophils
Basophils
14.2%
Lymphoid
B Cells
T Cells
NK Cells
Platelets
B
Blood
Spleen
Lymph Nodes
Bone Marrow
Peritoneum
BAL
Ly6G+ Neutrophils
Ly6C+ Monocytes
Ly6Clow Monocytes
SiglecF+ Eosinophils
DX5+mIgE+ Basophils
DX5+IgE+ Basophils
CD11bhi Macrophages
CD11chi Macrophages
mIgE+ CD117+ Mast Cells
CD19+IgM+ B Cells
CD19+ B Cells
B220+ B Cells
CD3+ T Cells
NKp46+ DX5+ NK Cells
CD41+ Platelets
VG1543
VG1505
C
donor 1
donor 2
donor 3
donor 4
Basophils
hFcγRIIA
VG1543 1
VG1543 2
VG1543 3
VG1543 4

Figure 3

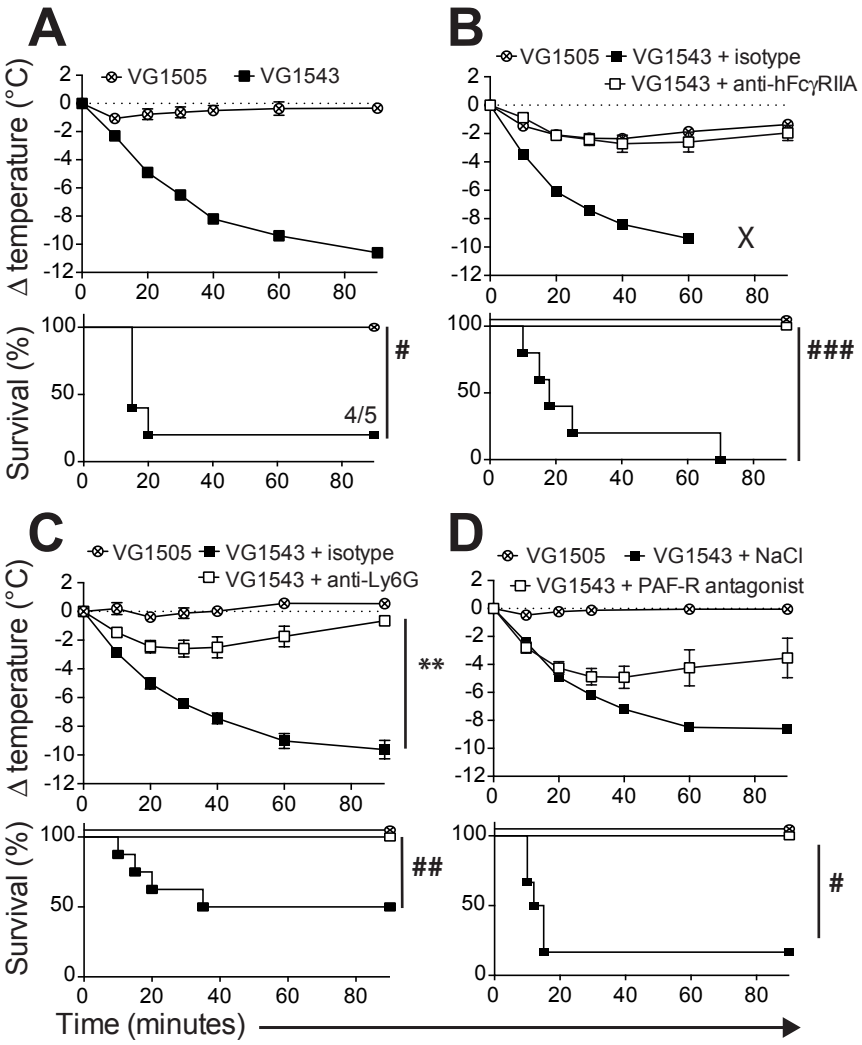
A
VG1505
VG1543
Δ temperature (°C)
Survival (%)
4/5
#
B
VG1505
VG1543 + isotype
VG1543 + anti-hFcγRIIA
X
###
C
VG1505
VG1543 + isotype
VG1543 + anti-Ly6G
**
##
D
VG1505
VG1543 + NaCl
VG1543 + PAF-R antagonist
#
Time (minutes)

Figure 4

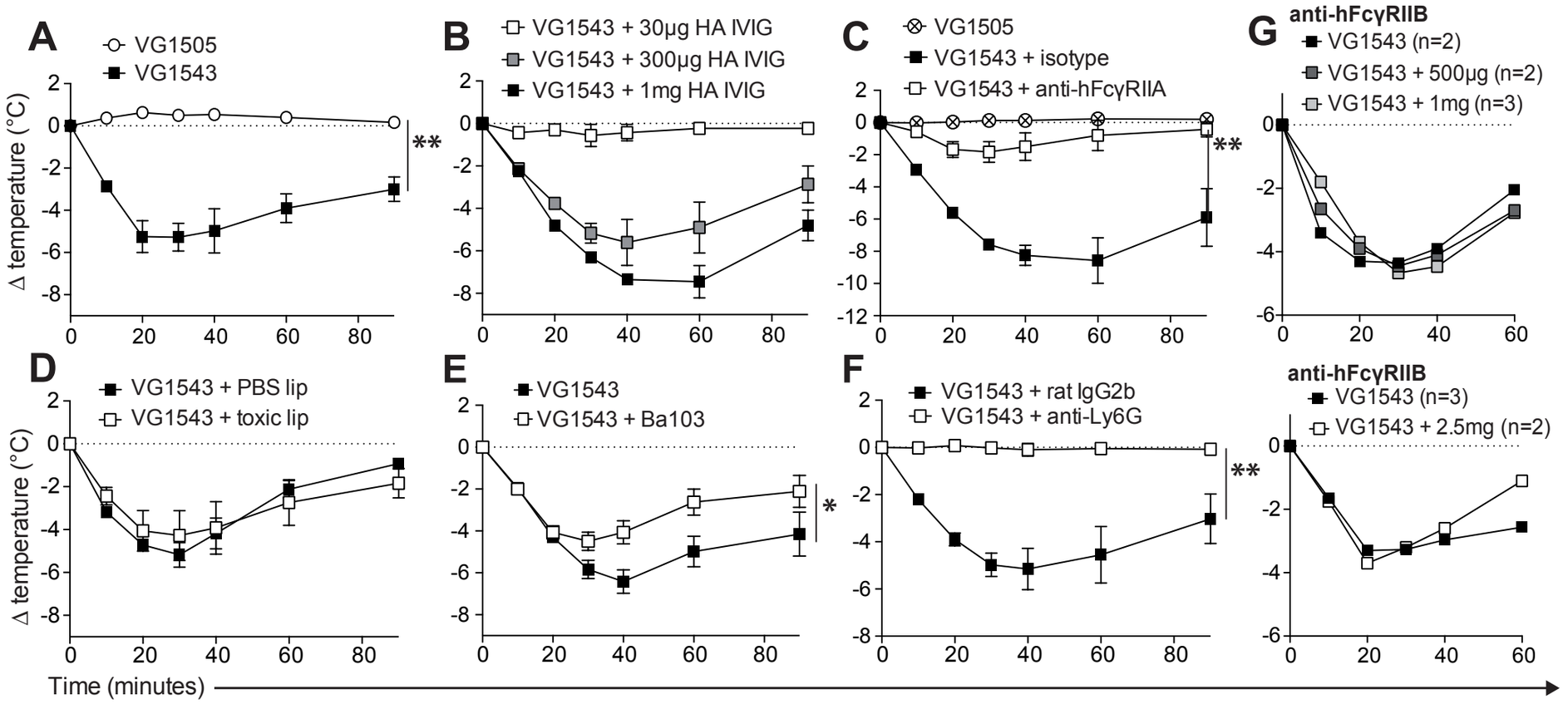
A
VG1505
VG1543
B
VG1543 + 30µg HA IVIG
VG1543 + 300µg HA IVIG
VG1543 + 1mg HA IVIG
C
VG1505
VG1543 + isotype
VG1543 + anti-hFcγRIIA
G
anti-hFcγRIIB
VG1543 (n=2)
VG1543 + 500µg (n=2)
VG1543 + 1mg (n=3)
D
VG1543 + PBS lip
VG1543 + toxic lip
E
VG1543
VG1543 + Ba103
F
VG1543 + rat IgG2b
VG1543 + anti-Ly6G
anti-hFcγRIIB
VG1543 (n=3)
VG1543 + 2.5mg (n=2)
Δ temperature (°C)
Time (minutes)
**
**
*

Figure 5

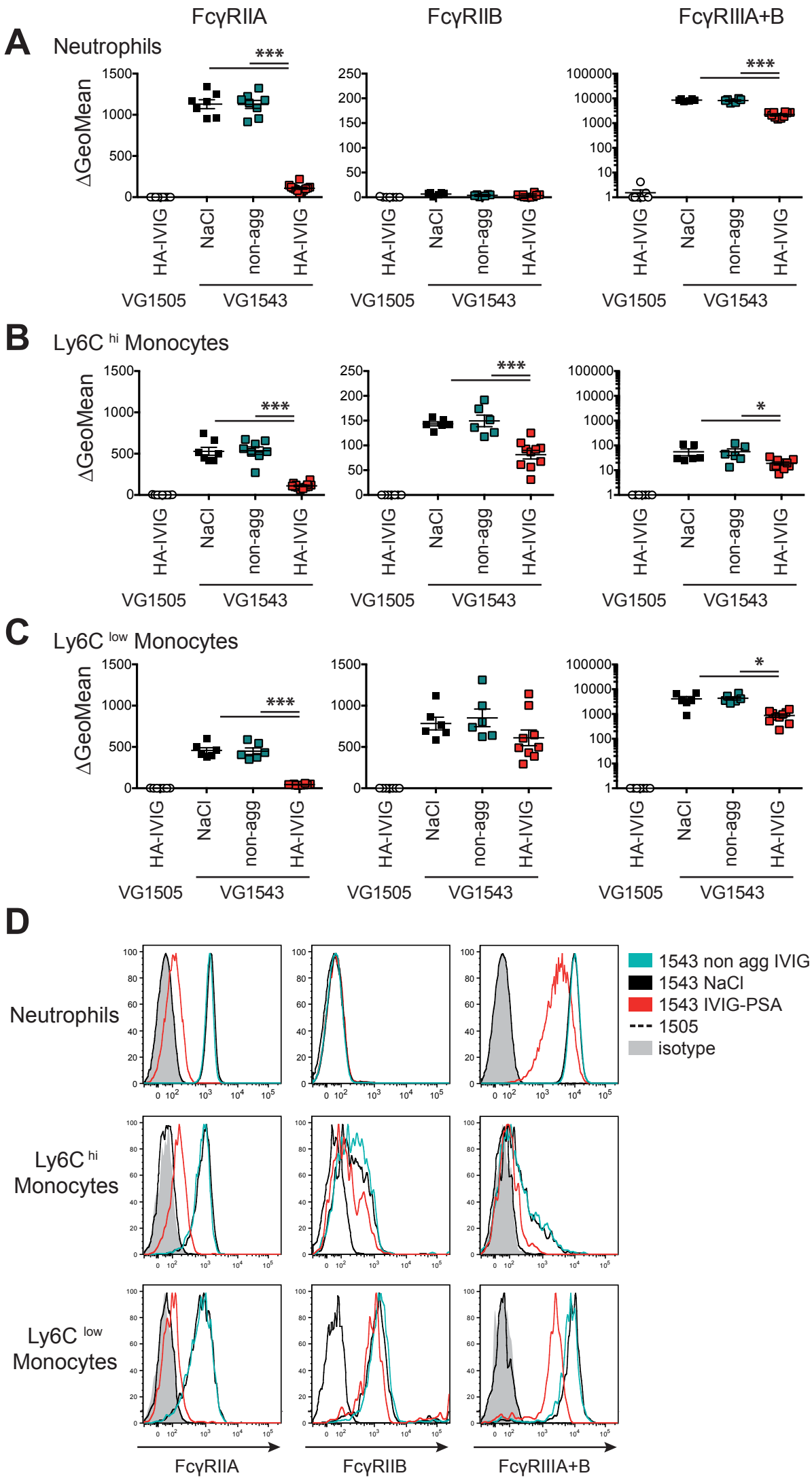
FcγRIIA
FcγRIIB
FcγRIIIA+B
A
Neutrophils
B
Ly6C hi Monocytes
C
Ly6C low Monocytes
ΔGeoMean
***
*
HA-IVIG
NaCl
non-agg
HA-IVIG
VG1505
VG1543
D
Neutrophils
Ly6C hi Monocytes
Ly6C low Monocytes
1543 non agg IVIG
1543 NaCl
1543 IVIG-PSA
1505
isotype
FcγRIIA
FcγRIIB
FcγRIIIA+B

Figure 6

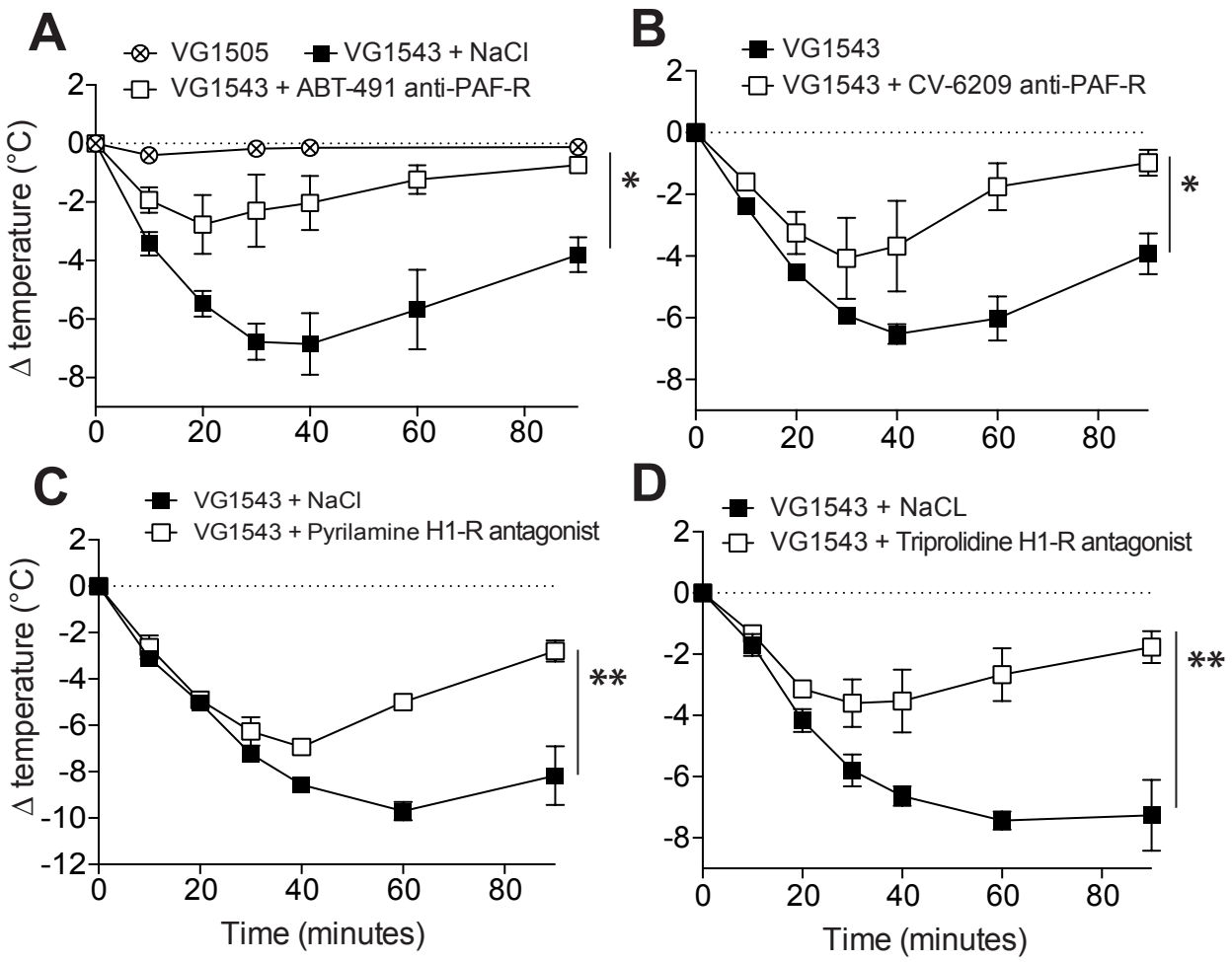
A
VG1505
VG1543 + NaCl
VG1543 + ABT-491 anti-PAF-R
Δ temperature (°C)
*
B
VG1543
VG1543 + CV-6209 anti-PAF-R
*
C
VG1543 + NaCl
VG1543 + Pyrilamine H1-R antagonist
Δ temperature (°C)
**
Time (minutes)
D
VG1543 + NaCL
VG1543 + Triprolidine H1-R antagonist
**
Time (minutes)

Supplementary Figure 1

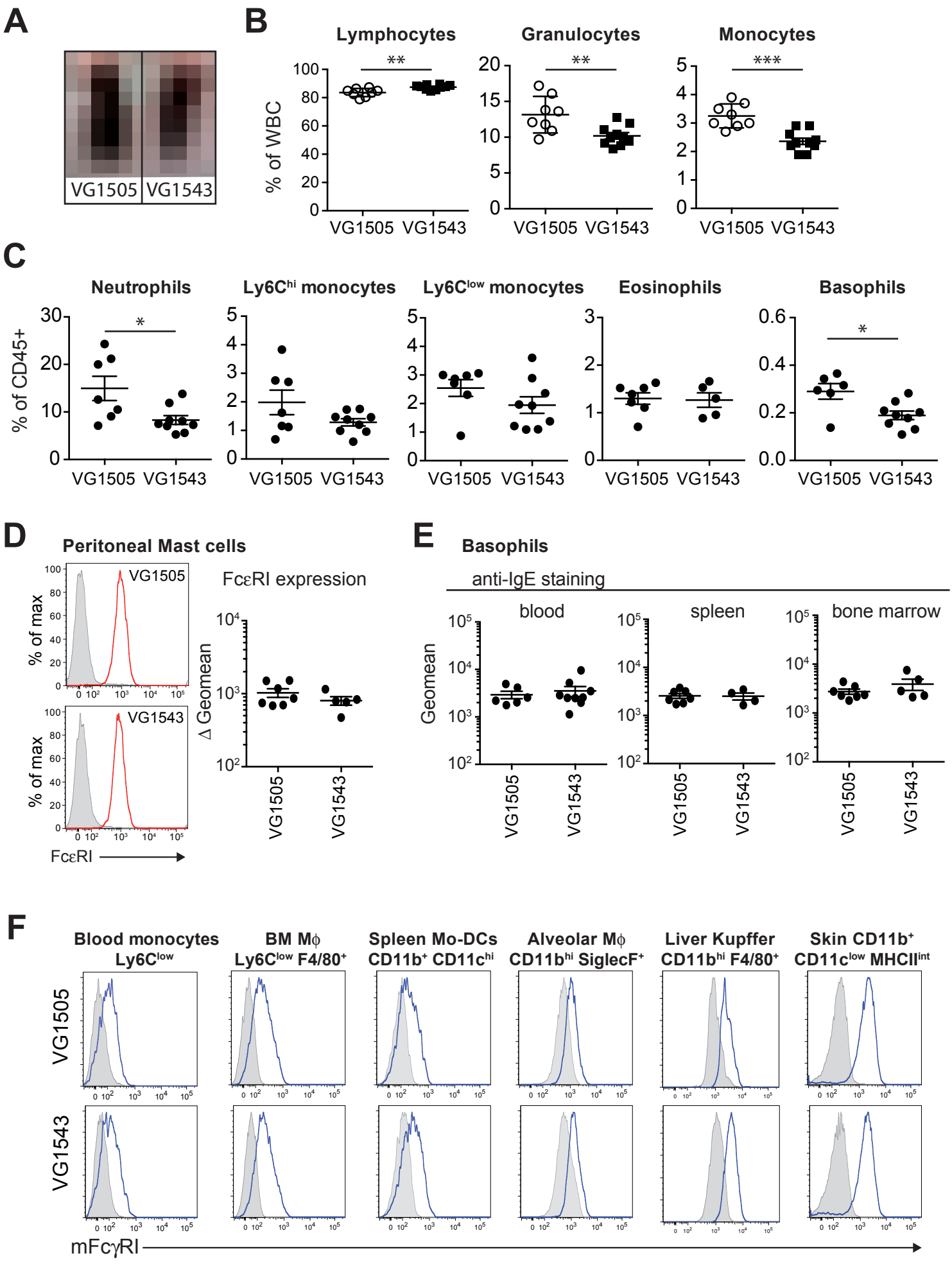

Supplementary Figure 2

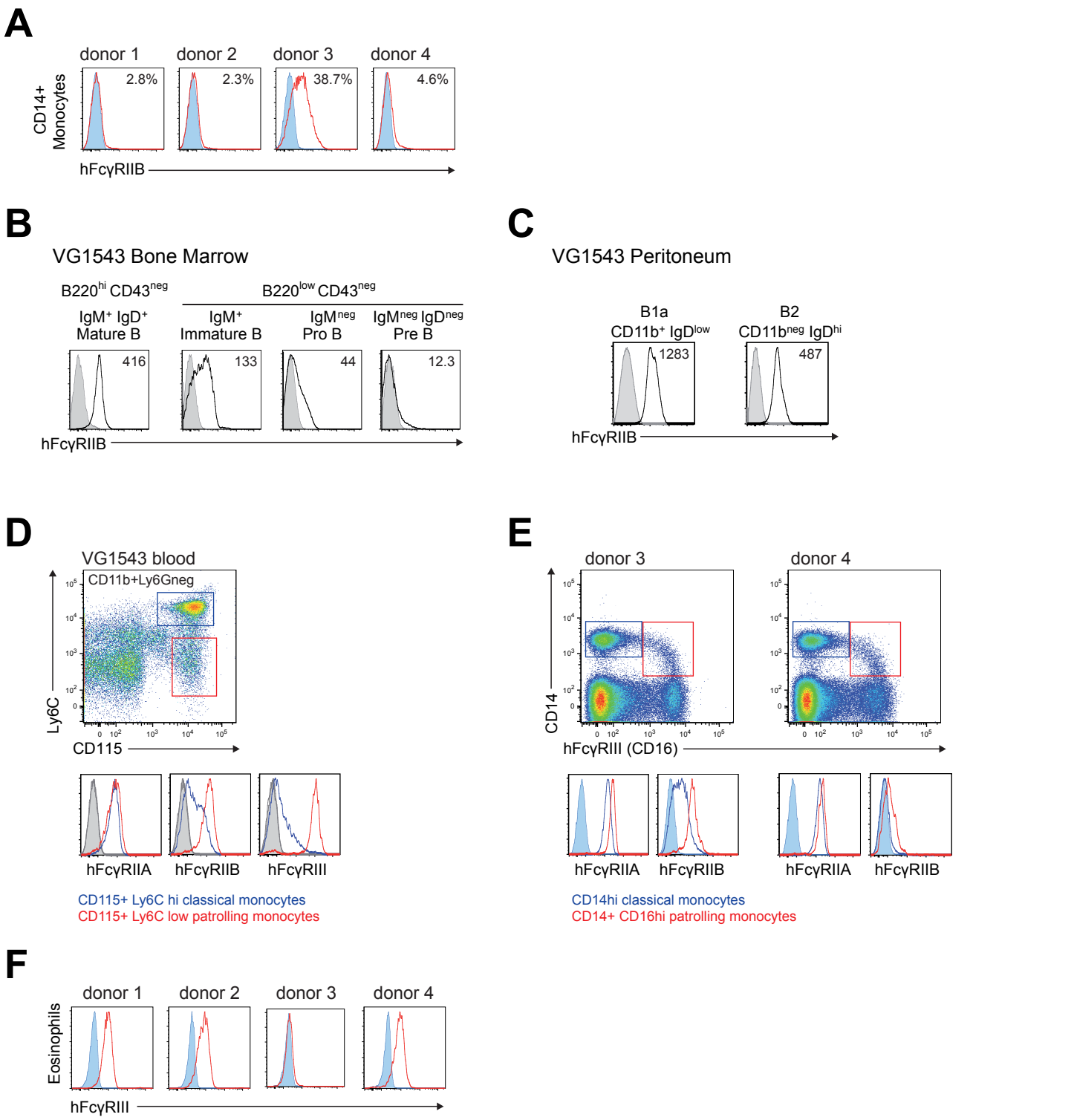

Supplementary Figure 3

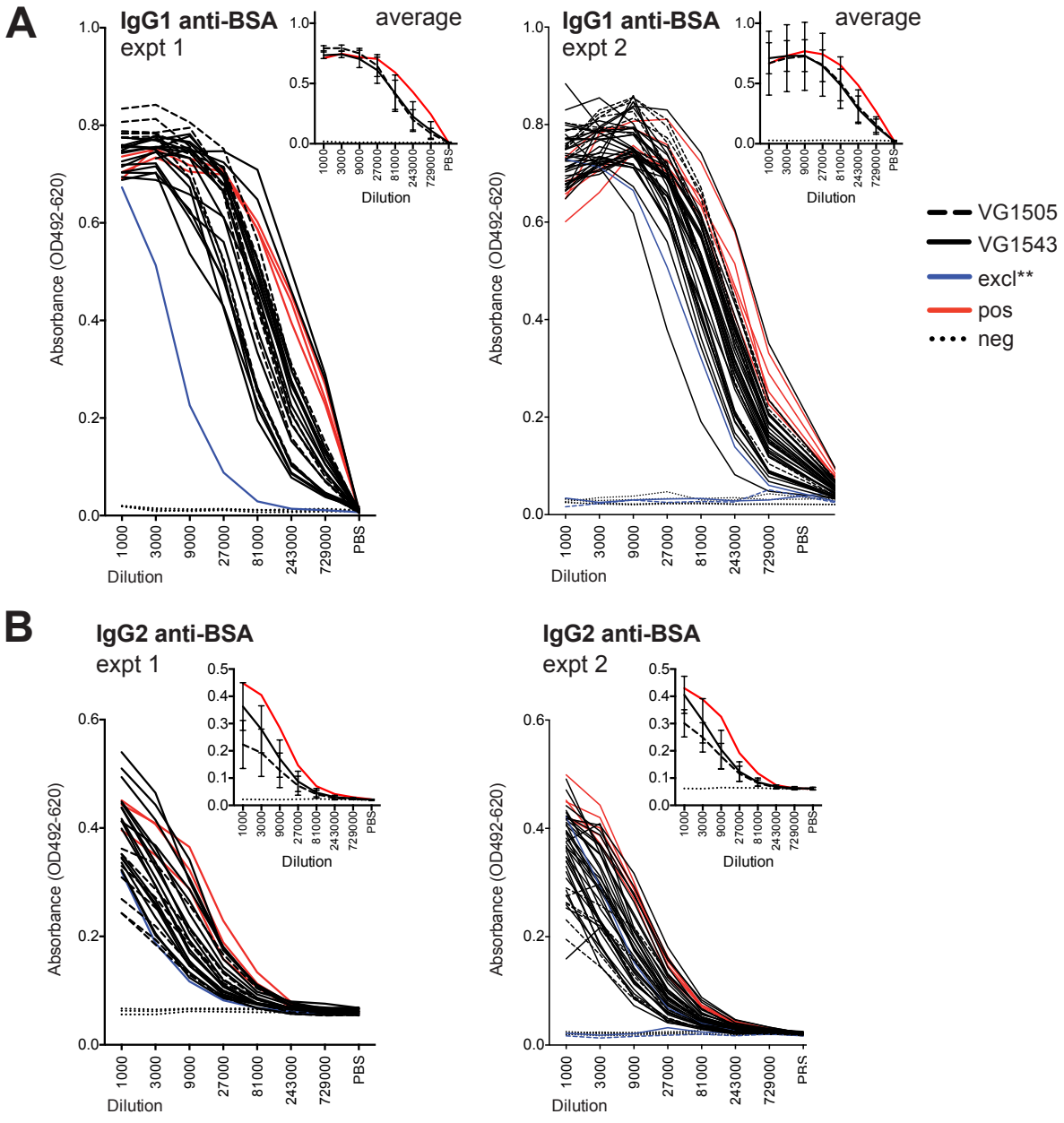

Supplementary Figure 4

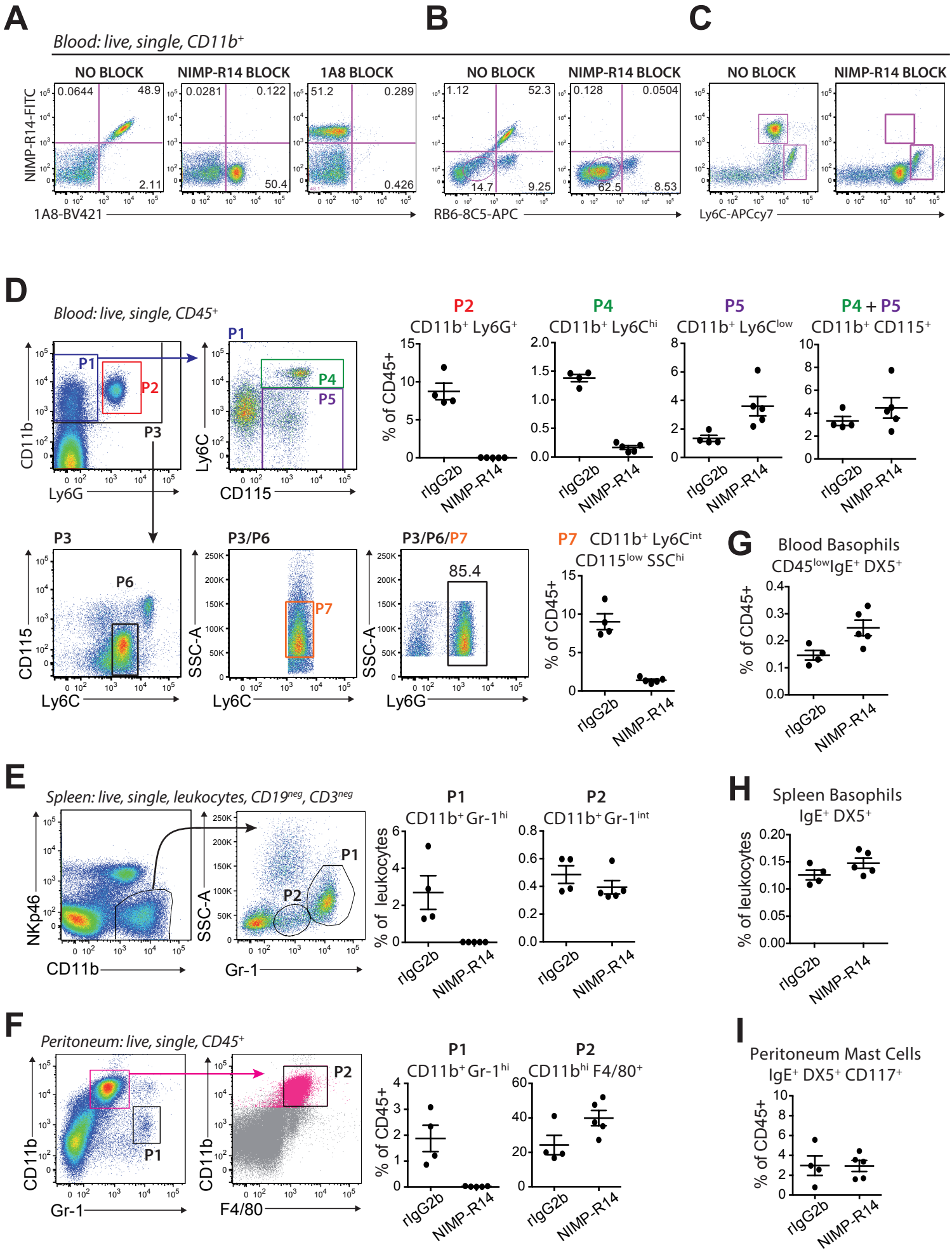

Supplementary Figure 5

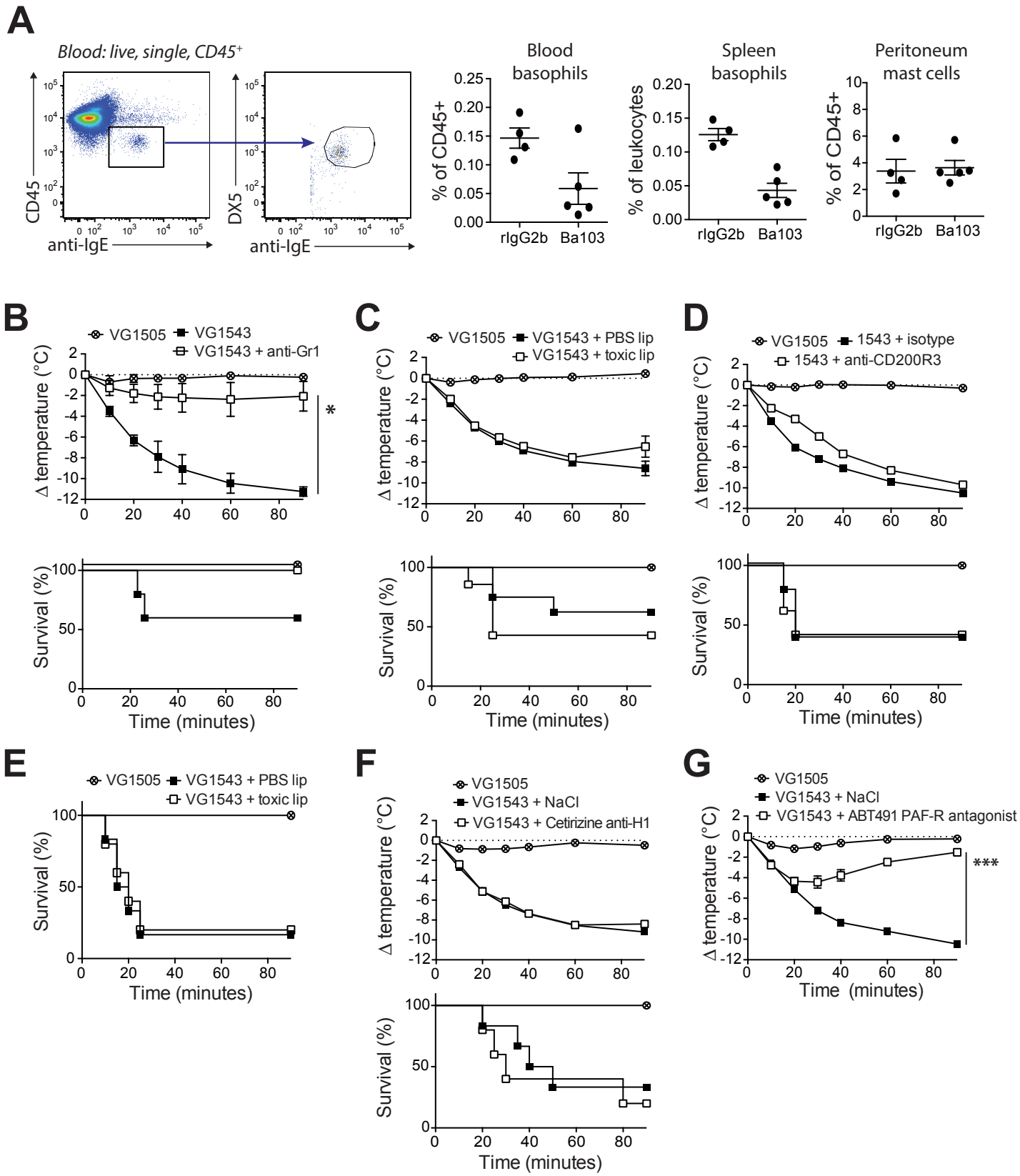

Supplementary Figure 6

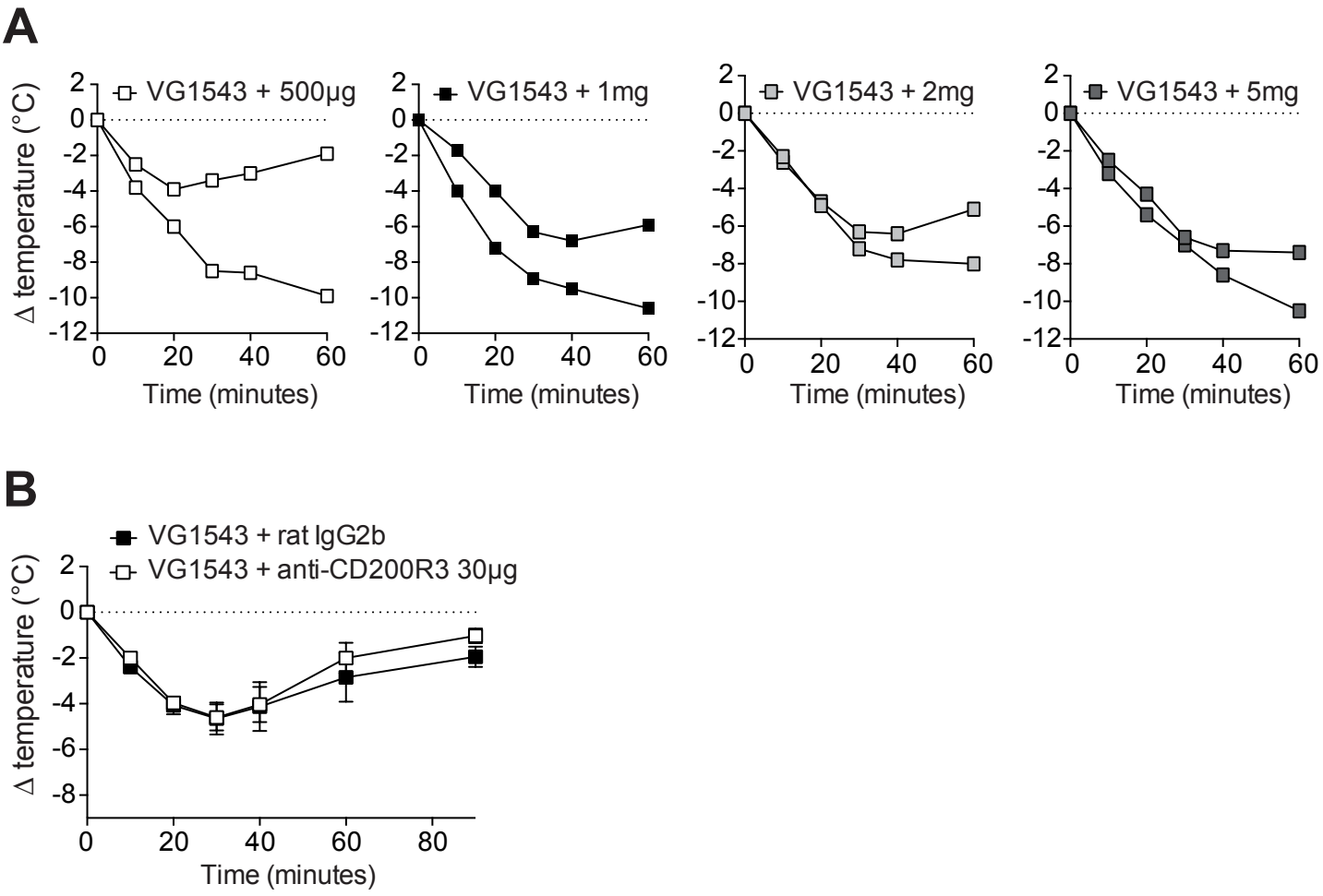

Supplementary Figure 7

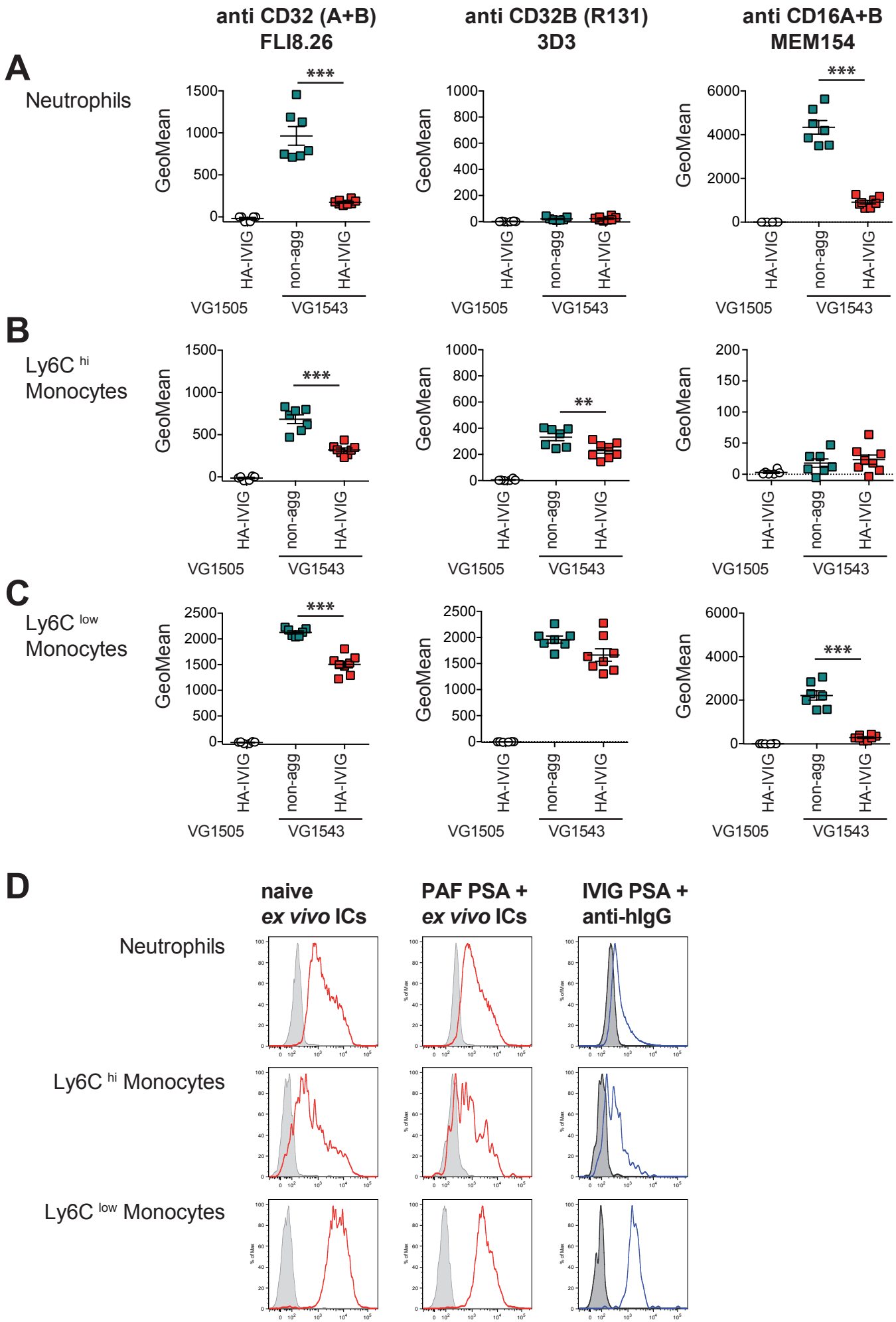

Supplemental Figure 8